RUTHENIUM AND OSMIUM COMPLEXES AS CATALYST PRECURSORS FOR FISCHER-TROPSCH SYNTHESIS

A thesis submitted to the

UNIVERSITY OF CAPE TOWN

in fulfilment of the requirements for the degree of

MASTER OF SCIENCE

by

NTOMBOVUYO BUNGANE

B.Sc (Hons) (Rhodes)

Department of Chemistry

University of Cape Town

Rhondebosch

South Africa

November 2004

PREFACE

The study of "Ruthenium complexes as catalyst precursors for Fischer-Tropsch synthesis" represents the original work by the author. Where use of the work of others has been made, it is duly acknowledged by means of reference.

Ntombovuyo Bungane

ACKNOWLEDGEMENTS

I would like to thank, first and foremost, the Lord Almighty for giving me strength to make it this far, you have shown me that nothing is impossible with you. My sincere gratitude and appreciation is also extended to my supervisors, Prof. J. R. Moss for his patience, support and enthusiasm throughout the course of this project, Dr. Claeys who has always made available his precious time to assist me with the catalytic experiments and Prof. van Steen for his guidance.

I am grateful to Mr P. Smith and Mr N. Hendricks for recording the NMR spectra and Mr P. Benin-Casa for carrying out the microanalyses. A special thanks goes to Rachel Cupido in the Department of Chemical Engineering for her help with the operation of the GC and also the technical staff.

My collegues and friends in the Chemistry Department have also contributed to this work, especially Dr P. Beagley who gave me insight and valuable assistance.

I would also like to thank the National Research Foundation (NRF) and the University of Cape Town for financial support.

My family has always been there for me through thick and thin, words cannot express how grateful I am for all their support and encouragement over my entire University career.

ABSTRACT

Ruthenium complexes of several types have been synthesized, supported on silica and their activity in CO hydrogenation was investigated in order to determine the cluster size of surface Ru atoms required for the formation of hydrocarbons. Previous studies have shown that more than one metallic site is needed for the Fischer-Tropsch synthesis.

In this study the bi-nuclear complexes that were synthesized are $[RuCp(CO)_2]_2$ $[RuCp^*(CO)_2]_2$ and $[Ru_2(CO)_2(\mu\text{-}CO)(\mu\text{-}CHMe)(\eta^5\text{-}Cp)_2]$. A comparative study was done with osmium complexes, since little work has been done in testing osmium for Fischer-Tropsch activity. The osmium analogue of the ruthenium complex $[CpRu(CO)_2]_2$ has been prepared ie $[CpOs(CO)_2]_2$. All complexes were characterized by IR, ^1H and ^{13}C NMR spectroscopy and microanalysis, and their properties are discussed. Fischer-Tropsch activity has been tested using a flow reactor. These new results are presented and discussed.

ABBREVIATIONS

Å	angstrom
ASF	Anderson-Schultz-Flory
bbl	barrel
br	broad (in NMR)
°C	degrees Celsius
Cp	cyclopentadienyl (η^5-C_5H_5)
Cp*	pentamethylcyclopentadienyl (η^5-$C_5(CH_3)_5$)
d	doublet (in NMR)
Eq	equation
Equiv.	equivalent
FID	flame ionisation detector
FT	Fischer-Tropsch
g	gram
GC	gas chromatograph
h	hour
HC	hydrocarbon
Hz	hertz
IR	infrared
m	medium (in IR)
Me	methyl (CH_3)
min	minute
mol	mol
m.p.	melting point
NMR	nuclear magnetic resonance
Ph	phenyl (C_6H_5)
ppm	parts per million
q	quartet (in NMR)
s	second
s	singlet (in NMR)
s	strong (in IR)
TCD	thermal conductivity detector

THF	tetrahydrofuran
TOS	time on stream
t	ton
voc	volatile organic compound (s)
w	weak (in IR)
wt	weight
y	year

TABLE OF CONTENTS

CHAPTER 1
INTRODUCTION TO THE FISCHER-TROPSCH PROCESS

1. Introduction

1.1 The Fischer-Tropsch process

Franz Fischer and Hans Tropsch discovered the synthesis of higher hydrocarbons by catalytic hydrogenation of carbon monoxide in 1926 [1]. The products range from gases such as methane, to liquid oil to solid wax. The Fischer-Tropsch synthesis occurs via the following chemical reaction:

$$CO + 2H_2 \rightarrow CH_2 + H_2O \qquad \Delta H_R\,(250^{\circ}C) = -158\ kJ/mol$$

with the CH_2 units subsequently being polymerised, forming a range of hydrocarbons. The reaction is highly exothermic and in order to obtain long chain hydrocarbons the temperature must be kept low. The consequence of higher temperatures is the selectivity of the undesired methane and also the increase of the rate of deposition of carbon, which may result in catalyst particle disintegration [2]. It was shown by Fischer and Tropsch that linear alkanes and alkenes, as well as some oxygenates, are formed at 200-300°C over iron or cobalt catalysts (Eq. (1) or Eq. (2)) [3]:

$$n\mathrm{CO} + (2n + 1)\,\mathrm{H_2} = \mathrm{C}_n\mathrm{H}_{2n+2} + n\mathrm{H_2O} \qquad (1)$$

or $$2n\mathrm{CO} + (n + 1)\,\mathrm{H_2} = \mathrm{C}_n\mathrm{H}_{2n+2} + n\mathrm{CO_2} \qquad (2)$$

The depletion of crude oil and thus the rise in price of crude oil has sparked interest in production of synthesis gas (H_2 + CO) from other sources e.g. methane, which is then converted to a range of fuels. Coal and methane (also known as natural gas) are the main raw materials for the production of synthesis gas. These have partially succeeded in replacing the crude oil, the conventional raw material. Biomass as starting material for FT also finds interest. Reserves for coal and natural gas are much larger than those for crude oil as shown in Table 1.1 below. Nowadays, Fischer-

Tropsch synthesis is seen as a method to access remote natural gas fields and to convert natural gas associated with oil fields [4]. In the latter case, Fischer-Tropsch synthesis is used as an environmentally benign route to avoid flaring.

Table 1.1 An estimate of the ultimate economic recoverable energy sources [2].

Source	Reserve (10^9 bbl oil equivalent)	Life (years) [a]
Tar Sands	1500	40
Oil	2000	50
Shale Oil	2500	65
Gas (methane)	3000	75
Coal	53000	1300

[a] At an annual energy demand of about $40 \cdot 10^9$ bbl oil per year.

The application of the FT process started in Germany and by 1938 there were nine coal-based plants in operation having a combined capacity of about 660 000 tons per year [4]. The plants were running mainly on iron.

During the 1950s another FT plant was built in Brownsville Texas with a capacity of about $360 \cdot 10^3$ t / y but was later shut down due to drastic increase in the price of natural gas. Not so long after that, a coal-based plant was built in Sasolburg (South Africa) as very little oil was available in this area but it had extensive coal deposits, which could be utilised to produce liquid fuels [5].

As a result of sharply rising crude oil prices in the 1970s, Sasol expanded its operations and the Sasol II and III plants came on stream in Secunda 1980 and 1982, respectively [2]. Large FT plants are currently operating in South Africa and Malaysia and are being built, or are in advance planning, by major multinationals, in Qatar, Nigeria, Egypt, Indonesia, and Australia; FT technology becomes competitive at an oil price of ca. US $25/barrel [6] and even lower.

1.2 Synthesis gas production

All Fischer-Tropsch processes require synthesis gas (H_2 +CO) as the feedstock. The production of synthesis gas is achieved through three processes or combinations thereof [7]:

- Steam reforming,
- Carbon dioxide reforming, and
- Partial oxidation.

Methane reforming is preferred to coal gasification for synthesis gas production because only about 20% of the carbon is converted to CO_2. Coal gasification is an inefficient process, with approximately 50% carbon loss due to the formation of CO_2 [2]. The reformation of methane is more efficient, with approximately 70% carbon conversion to CO [2]. It is therefore not surprising why most FT plants use methane as the source of synthesis gas. The production of synthesis gas having H_2 and CO in the ratio 2:1 the required overall reaction stoichiometry can be represented as follows [2]:

$$1.11CH_4 + 0.72O_2 \rightarrow 2H_2 + 1CO + 0.11CO_2 + 0.22\,H_2O \quad (1)$$

$$1.78CH_{0.5}(coal) + 0.50O_2 + 1.56H_2O \rightarrow 2H_2 + 1CO + 0.78CO_2 \quad (2)$$

1.3 Catalysts in FT synthesis

The most commonly used catalysts in FT synthesis are cobalt-, nickel-, iron- and ruthenium-based [8], with the latter being the most expensive due to its limited supply reserves. On a relative basis taking the price of scrap iron as 1.0, the approximate cost of Ni is 250, of Co is 1000 and of Ru is 50 000 [4]. Nickel produces too much methane and thus, on commercial scale, iron and cobalt are used.

The original German plants used Co catalyst due to its higher activity and longer life span. However, Fe is not only cheaper but it can produce more olefins, which are valuable petrochemical feedstocks. Cobalt and ruthenium catalysts have been studied

extensively due to their high activity in FT synthesis. All these FT catalysts have common properties, such as their activity in hydrogenation reactions and capability for metal carbonyl formation [26].

In this work, ruthenium and osmium were used as catalyst precursors for the FT reaction. These two platinum group metals are both rare and expensive, which limits their industrial application. As mentioned earlier, ruthenium is well known for its high FT activity and selectivity. In addition, when compared to other catalysts it is the least complicated with respect to carbide or oxide formation. At low temperatures and high pressures the formation of carbonyls can be expected. At low temperatures (<150°C) and high synthesis gas pressures (>100 bar), it produces high molecular weight hydrocarbons and this clearly indicates its ability to perform chain growth in its "cleanest" mode and therefore providing the simplest catalytic system of FT synthesis where mechanistic conclusions should be easiest [9].

Osmium, on oxidation, tends to form an oxide (OsO_4), which is quite toxic. However, Choplin and Leconte [49] have reported their results on the FT synthesis of a bimetallic $H_2FeOs_3(CO)_{13}/SiO_2$ catalyst and they compared these results with those obtained with catalysts derived from $Fe_3(CO)_{12}/SiO_2$ and $Os_3(CO)_{12}/SiO_2$. Their findings revealed that all three catalysts are active in the FT synthesis and they are selective towards C_1-C_4 hydrocarbons. Addition of Fe to the Os system decreases methane selectivity and it increases the propagation to C_2-C_4 hydrocarbons.

Currently, about 85% of all industrial processes are carried out using heterogeneous catalysts [10,11], for example, Sasol uses a heterogeneous Fe catalyst in chain FT reactions at present. Heterogeneous catalysts have high stability to temperature and can be easily separated from reaction products whereas, in contrast, homogeneous catalysts are difficult to separate from reaction products and it is quite expensive to regenerate such catalysts for re-use. In comparison to homogeneously catalysed reactions, the mechanisms of heterogeneous catalytic reactions are difficult to understand due to the complexity of the catalyst surface. The FT processes, which are heterogeneously catalysed, involve the formation, presumably by quite different paths, of several different types of products of which many of these arise by

secondary reactions from primary products [3]. Since the primary and secondary products appear to be formed simultaneously, under some conditions, it is sometimes difficult to distinguish between the two. Table 1.2 shows the advantages and disadvantages of homogeneous and heterogeneous catalysts [12].

Table 1.2: Advantages and disadvantages of homogeneous and heterogeneous catalysts [12].

	Homogeneous Catalysis	**Heterogeneous Catalysis**
Activity	high	variable
Selectivity	high	variable
Reaction conditions	mild	harsh
Catalyst life	variable	long
Sensitivity toward catalyst poisons	low	high
Diffusion problems	none	may be important
Catalyst recycling	expensive	not necessary
Variability of steric and electronic properties of catalyst	possible	not possible
Understanding of mechanism	fairly good	very poor (except for model systems
Product separation	difficult	easy

1.3.1 Methods of preparation of the catalysts

The characteristics and the performance of FT catalysts depend greatly on the precursor used together with the method of preparation as well as the pre-treatment procedures [13]. For instance, cobalt catalysts are prepared from salt precursors by pH controlled precipitation or incipient wetness impregnation (IWI) technique. It has been reported by Reuel and Bartholomew [14] that a precipitated 3 wt% Co/SiO_2 catalyst exhibits a significantly lower extent of reduction and lower hydrogen uptake than its impregnated counterpart, a result perhaps due to the more intimate contact of cobalt with silica in conjunction with precipitation and this was indicated by observation that the precipitated catalysts generally have a narrower crystallite size distribution than impregnated ones [13]. The implication of this observation is that the precipitated 3wt % catalyst is less active in CO hydrogenation than the impregnated catalyst.

1.4 Metal carbonyl complexes as precursors

The use of catalysts prepared from organometallic metal carbonyl precursor complexes in catalysis is perhaps one of the most interesting applications of these cluster complexes. Studies have shown that catalysts prepared from metal carbonyl precursor complexes show much greater metal dispersion than similar catalysts prepared from metal salt solutions [15]. This is due to the active metallic phase, which consists of extremely small particles, which results in higher degree of dispersion. These particles do not readily coalesce or sinter because they are firmly anchored to the surface and are widely separated from each other [16].

Not only do the catalyst which are derived from metal carbonyl precursor complexes give rise to well defined metal loadings, they also contain metals in low oxidation states and their decomposition enables pre-reduced metals to be obtained, which facilitates the use of milder catalyst activation conditions [15]. However, the air sensitivity of many supported metal carbonyl complexes leads to difficulties in the handling and preparation procedures.

1.4.1 Ruthenium complexes as catalyst precursors

Ruthenium compounds are widely used as homogeneous catalysts; for example, $RuCl_2(PPh_3)_3$ is a useful catalyst for the hydrogenation of carbon-carbon double bonds [16]. However, the hydrogenation of aldehydes to alcohols is catalysed by $Ru(CO)_3(PPh_3)_2$ [17]. There are also quite a number of other reactions of ruthenium complexes and these include hydroformylation [17], polymerisation of ethylene [18], hydrogen / deuterium exchange [19] and hydrogenation of CO_2 to formic acid in supercritical carbon dioxide [20], to mention a few. Grubbs et al [52] have recently made some important new discoveries concerning a class of catalysts, specifically, ruthenium-alkylidene olefin metathesis catalysts, which are able to catalyse reactions such as ring-closing metathesis of dienes, ring-opening cross metathesis of olefins and ring-opening metathesis polymerisation. These catalysts react selectively with olefins in the presence of proton-bearing solvents as well as polar functional groups [53].

Ruthenium fixed on supports such as SiO_2, Al_2O_3, MgO, TiO_2 and zeolites have been tested as heterogeneous catalysts [21]. These supports have a high surface area, which makes it easier for the metals to be dispersed over the surface. Supported metals are effective catalysts as the active metallic phase consists of extremely small particles [22]. The preparation of the heterogeneous catalysts is fairly simple and is for example carried out by first impregnating the support with a ruthenium salt (eg. $RuCl_3 \cdot xH_2O$) dissolved in water. The solvent is then removed by drying the catalyst at a certain temperature for a certain period of time and this is followed by reduction with e.g. hydrogen at temperatures between 300 and 400°C. The end result is the formation of the metallic Ru on the surface of the support.

Decomposition of adsorbed $Ru_3(CO)_{12}$ at elevated temperatures has also been proven to be another effective way to facilitate the anchoring of metallic ruthenium on oxidic supports [21]. These ruthenium catalysts anchored on supports not only play a vital role in Fischer-Tropsch synthesis but they are also used in the hydrogenation of C=C double bonds [23]. They are also known to reduce benzene to cyclohexane [24] or even selectively to cyclohexene [25].

1.5 Reaction mechanisms

The conversion of the CO/H_2 mixture into product molecules, which consist of different chain lengths, is thought to be a multi-step reaction. From the equation:

$$CO + 2H_2 \rightarrow (CH_2) + H_2O$$

the following reactions occur [26]:

- adsorption of CO
- splitting of the C/O-bond
- dissociative adsorption of $2H_2$
- transfer of 2H to the oxygen to yield H_2O
- desorption of H_2O
- transfer of 2H to the carbon to yield CH_2
- formation of a new C/C-bond
- desorption of products

Since the reaction intermediates remain firmly anchored on the catalyst surface, in other words, they are not desorbed from the surface, the conversion of H_2 and CO is perceived as a one step reaction. The question as to whether the formation of the oxygen containing intermediates is achieved by adding the hydrogen to the adsorbed CO first or the C/O-bond splits first, thereby producing hydrocarbon intermediates, still remains. As a result of this uncertainty, a few mechanisms have been proposed in order to try and explain the formation of the FT products.

1.5.1 The Methylene Insertion mechanism

Scheme 1 shows a detailed pathway of the methane formation according to the Methylene Insertion mechanism. The mechanism was originally stated by Fischer and Tropsch in 1926 and was later put forward by Pettit and Biloen and their co-workers [27,28]. This theory, which included the formation of metal carbides, was discarded since no carbide phases were discovered with cobalt and ruthenium as the catalysts [29]. According to the mechanism the CO is coordinated and activated on

the metallic site, followed by C-O cleavage and hydrogenation to give sequentially surface carbide ($C_{(ad)}$), methylidyne ($CH_{(ad)}$), and methylene ($CH_{2(ad)}$) species [6]. The latter could then be further hydrogenated to surface methyl ($CH_{3(ad)}$) and finally released as methane [6].

Another approach (Scheme 2), which is, in essence, the same as Scheme 1, involves polymerisation of the surface methylenes to yield linear hydrocarbons, which is the FT reaction and a popular mechanism for this is the alkyl CH_2-insertion (alkyl + $\{CH_{2(ad)}\}$) scheme which involves the addition of CH_2 to alkyl chains which are initiated by a surface methyl) [6]

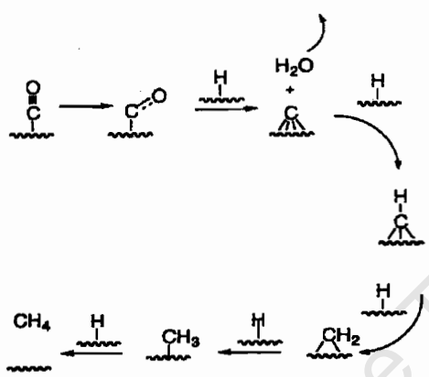

Scheme 1: Methane formation according to the Methylene insertion mechanism [6].

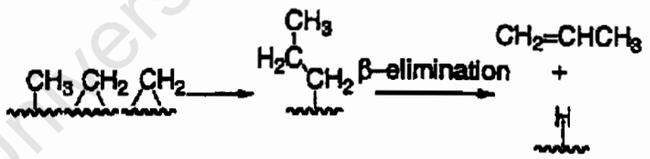

Scheme 2: Polymerisation of methylenes to yield linear hydrocarbons [6].

However, several alternative proposals have been made leading to the alkenyl + $\{CH_{2(ad)}\}$ mechanism (Scheme 3) [30]. In this mechanism it is believed that the chain

carriers are surface alkenyl species rather than alkyl species that react with methylenes.

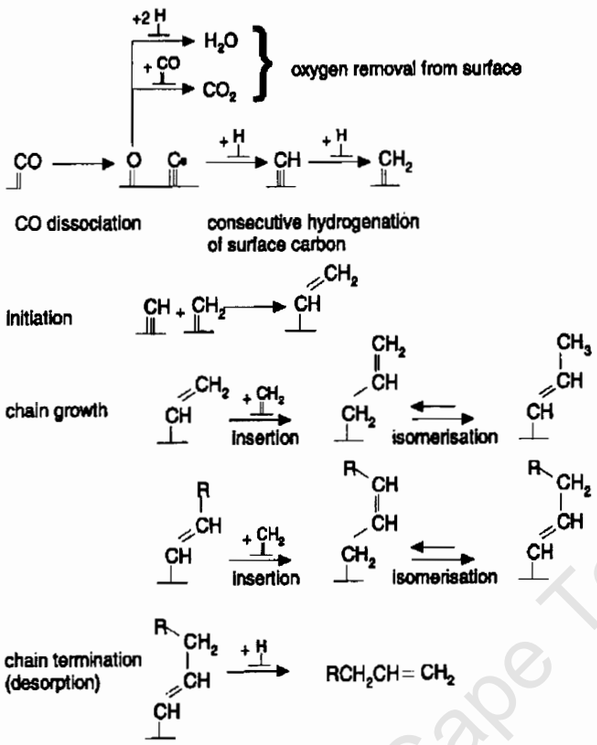

Scheme 3: Chain growth and product formation according to Maitlis et al. [31].

It is proposed, in this mechanism, that dissociation of chemisorbed CO and subsequent hydrogenation of the surface carbon yields surface methyne (≡CH) and surface methylene (=CH_2) species occurs, which then react further to form a surface vinyl species (-CH=CH_2) which is the chain starter [31]. The surface methylene species reacts with the vinyl species in a step-wise polymerisation to allow chain growth and an allyl species (-CH_2CH=CH_2) is eventually formed which can then isomerise to an alkyl species. According to this mechanism, the primary selectivity for *n*-paraffins is 0 mol% meaning that only α-olefins are formed as the primary product [31].

It was found that the associative desorption of an alkyl species with a chemisorbed hydrogen atom to form a paraffin is strongly inhibited compared to dissociative adsorption as an olefin as illustrated in Scheme 4.

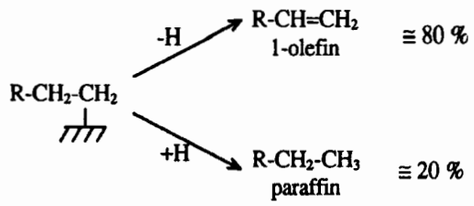

Scheme 4: Product formation via desorption of surface alkyl species and relative fractions of olefins and paraffins.

1.5.2 CO Insertion mechanism

Pichler and Schulz [32] suggested the CO insertion mechanism where chain growth is achieved by insertion of chemisorbed CO into the surface alkyl chains, which is bonded to the surface of the catalyst. Scheme 5 shows schematically chain growth and product formation according to the CO-insertion mechanism.

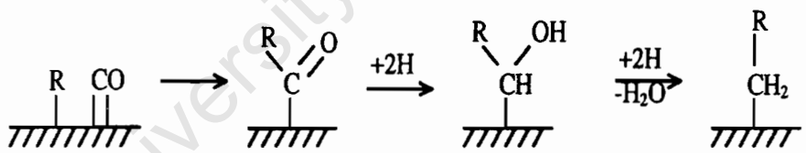

Scheme 5: Chain growth according to the CO-insertion mechanism [32].

The above mechanism accounts for the formation of oxygenates.

1.5.3 Enol condensation mechanism

In 1951, Storch, Golumbic and Anderson [55] proposed a mechanism whereby the chain growth process is promoted by the condensation of enolic surface species. Scheme 6 shows schematically chain growth and product formation according to the enol mechanism. This mechanism involves the chemisorption of CO, which reacts with adsorbed hydrogen to form a species such as [33]:

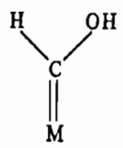

This enol group condenses as shown in Scheme 6.

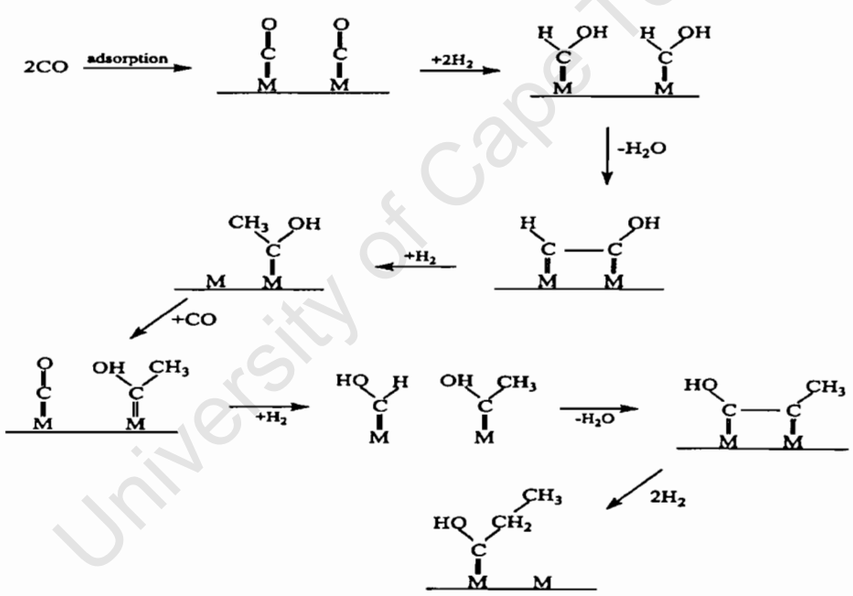

Scheme 6: Chain growth and product formation according to enol mechanism [33].

1.6 Product distribution in FT synthesis

The FT synthesis product spectrum consists of a multicomponent mixture of hydrocarbons. 1-Olefins are produced as a major primary product on iron catalysts, whereas *n*-paraffins are also formed directly but to a much lesser degree than 1-olefins which can be reincorporated into growing chains, hydrogenated or isomerised to 2-olefins [34]. Oxygenates (alcohols, aldehydes, acids and ketones) are also formed irrespective of operating conditions as well as branched products, almost exclusively methyl-branched, but only to a lesser extent. As the carbon number increases, the product yield decreases according to the Anderson-Schulz-Flory (ASF) distribution (Eq. (1)) [56]:

$$\log (W_n / n) = n \log \alpha + \log ((1- \alpha)^2 / \alpha) \quad (1)$$

where W_n = mass fraction of product

n = number of carbon atoms in hydrocarbon chain

α = chain growth probability

The chain growth probability, α, is greatly dependant on the temperature, pressure, type of catalyst and CO/H_2 ratio. Theoretically, the plot of log (W_n / n) against n gives a straight line with a slope of log α (Figure 1).

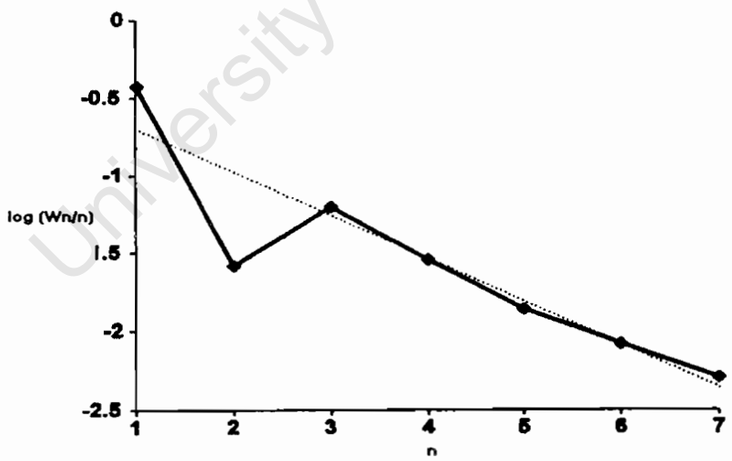

Figure 1: A plot of log (W_n/n) against n illustrating the ASF distribution [30].

However, in real FT product distributions often deviations from this ideal distribution are observed, in particular for methane, C_2, and higher molecular weight products [34-39]. Iglesia et al. [39] interpreted these deviations from the simple ASF distribution (for synthesis on ruthenium and cobalt) by readsorption of 1-alkenes and secondary chain propagation. However, Patzlaff et al. [40] concluded that for iron and cobalt catalysts the deviation from the ASF distribution is the result of superposition of two ASF distributions caused by different mechanisms of chain growth.

1.7 Variables that affect product distribution

The parameters that influence product distribution are temperature, partial pressure and catalyst type.

1.7.3 Effect of temperature

As the temperature is increased the probability of chain growth decreases and hence a shift in selectivity towards lower carbon number products and to more hydrogenated products is observed. This is presumably due to the increased rate of hydrogenation of the individual CH_2 units (to CH_3 and CH_4) thus lowering the surface concentration of CH_2 units [2]. As the chain length decreases, the degree of branching notably increases. The rate of deposition of carbon also increases with temperature, which can result in catalyst deactivation [29].

1.7.4 Effect of partial pressures

Lowering the partial pressure of CO results in the decrease in surface coverage by the CH_2 species, which lowers the probability of chain growth thus increasing the probability of desorption of the alkyl species [2]. However, termination of the surface species to paraffins occurs as the partial pressure of H_2 rises.

1.7.5 Effect of catalyst type

The key role of a catalyst is to increase the rate of a chemical reaction, as it is generally known. Under FT conditions, nickel produces too much methane, which makes it an unsuitable catalyst. Cobalt, ruthenium and iron are more effective catalysts [2]. The former produces more methane and less olefins when compared to the latter, which requires promotion by alkalis and thereby increasing the probability of chain growth as the basicity increases. In choosing the right catalyst, the chemical nature of the catalyst's surface and the geometrical structure of the catalyst crystals are of utmost importance.

1.8 Scope of thesis

The formation of higher hydrocarbons from CO and H_2 requires the adsorption of H_2 and CO, the cleavage of the H-H and the C-O bond, the hydrogenation of carbonaceous surface species, the removal of surface oxygen species, the formation of the C-C bond, and the desorption of the long chain alkyl species [54]. Claeys et al. have done previous work in an attempt to investigate the minimum ensemble size required for the Fischer-Tropsch synthesis, [44, 54]. They tested a mono-atomic ruthenium dendrimer as well as bi- and tri-nuclear complexes and from their findings they concluded that a single metallic site is not sufficient for the FT synthesis.

The work presented in this thesis, therefore, investigates the behaviour of the ruthenium complexes and their osmium analogues, specifically the bi- and tri-nuclear complexes on CO hydrogenation. The aim of this work is to observe if changing the ligands has any effect on the FT activity.

From the literature survey, it appears that not much work has been done on osmium to investigate its activity in Fischer-Tropsch synthesis. We therefore took the challenge to test whether osmium is active in CO hydrogenation or not. If so, is it more or less active than ruthenium?. This study, therefore, provides a comparison of the activity of the ruthenium and osmium complexes in Fischer-Tropsch synthesis.

CHAPTER 2

RESULTS AND DISCUSSION: EXPERIMENTS WITH RUTHENIUM

2.1 Introduction

Ruthenium is the most expensive and least abundant of all the metals that are most active in the Fischer-Tropsch synthesis, namely iron, cobalt and nickel [8]. Not only is ruthenium fundamentally important in CO hydrogenation reactions, it also plays a vital role in organometallic chemistry. Thus it forms organometallic complexes with CO, H_2 and hydrocarbons including cyclopentadienyl (Cp) ligands. The Cp ligands can be used as bridging systems to obtain dinuclear complexes [41]. The hydrogen in the Cp ligand can be substituted, for example, by methyl groups resulting in a bulkier Cp* ligand (where Cp* = pentamethylcyclopentadienyl) which changes the steric and electronic properties as well as the solubility of the transition metal complexes.

In an attempt to investigate the minimal ensemble size required for the Fischer-Tropsch reaction, previous work by Claeys et al. [44] has shown that mono-atomic ruthenium, using a dendrimer (Ru-Rp3G1C) (Figure 2.1) which contains ruthenium atoms on the periphery, is unable to catalyse the reaction. A dendrimer was used because of the high volatility of ruthenium carbonyl (e.g. $Ru(CO)_5$) under typical FT conditions.

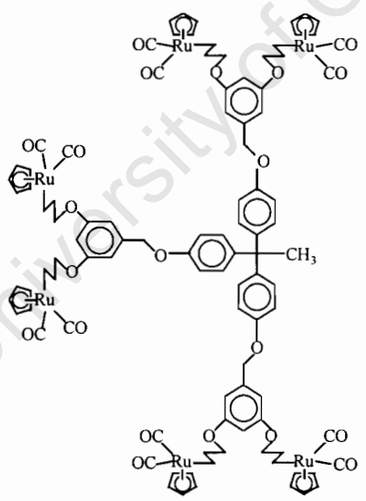

Figure 2.1: Structure of the ruthenium dendrimer (Ru-Rp3G1C).

In the work described in this thesis, the dinuclear ruthenium complexes $[CpRu(CO)_2]_2$ (**1**), $[Cp^*Ru(CO)_2]_2$ (**2**) and $[Ru_2(CO)_2(\mu\text{-}CO)(\mu\text{-}CHMe)(Cp)_2]$ (**3**), were synthesized by literature procedures and their activity in Fischer-Tropsch synthesis was investigated. However, an attempt to synthesize a novel dendrimer similar structurally to the Ru-Rp3G1C dendrimer but with dinuclear Ru-Ru units on the periphery of the dendrimer was unsuccessful.

The compounds were prepared according to literature methods and only $[CpRu(CO)_2]_2$ (**1**) has previously been tested for FT activity [44]. Figure 2.2 shows the Ru-complexes that have been prepared.

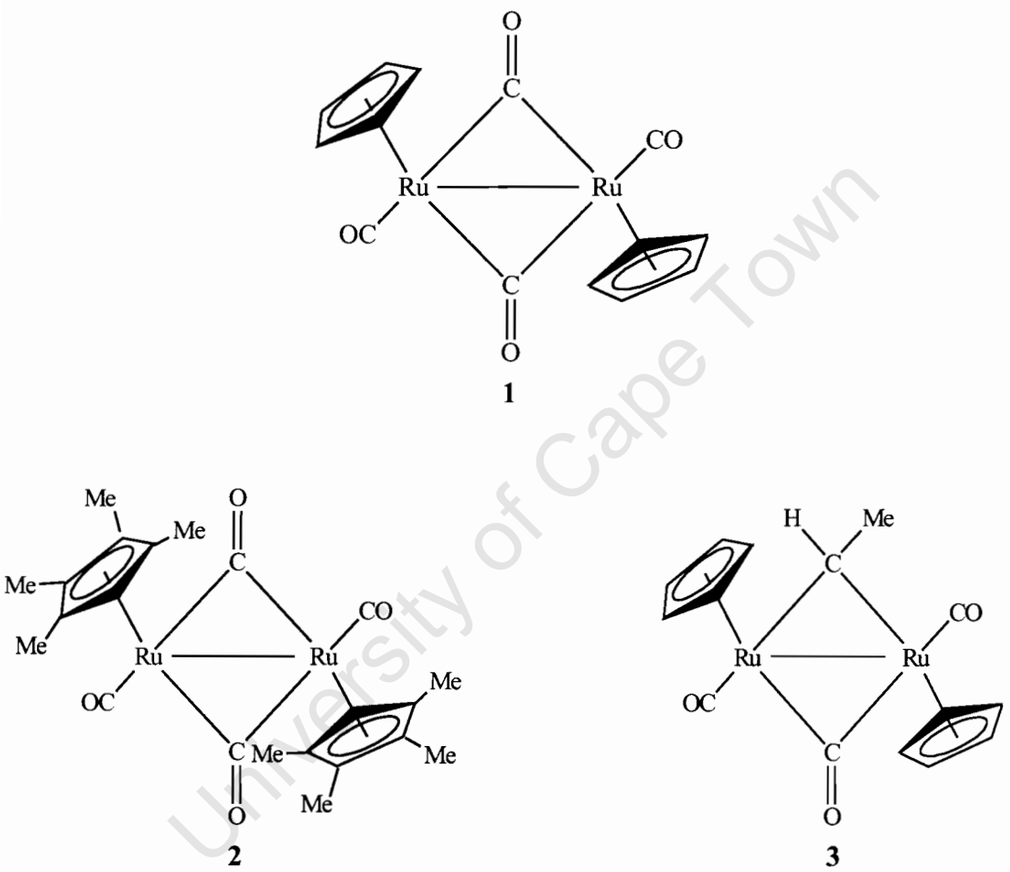

Figure 2.2: Structural representations of the compounds **1**, **2** and **3**.

2.2 Synthesis of compounds 1, 2 and 3

The synthesis of $[CpRu(CO)_2]_2$ (**1**) was performed by following Knox and Doherty's two-step procedure [42], which starts with the cracking of dicyclopentadiene over iron filings to obtain cyclopentadiene. It is followed by a further reaction of cyclopentadiene with triruthenium dodecacarbonyl in the presence of heptane and then refluxing the mixture for two hours (Eq. 1).

$$2/3[Ru_3(CO)_{12}] + 2C_5H_6 \longrightarrow 2[RuH(CO)_2(\eta^5\text{-}C_5H_5)] + 4CO \qquad \text{Eq.1}$$

Oxidation of the hydride afforded $[CpRu(CO)_2]_2$ (Eq. 2).

$$2[RuH(CO)_2(\eta^5\text{-}C_5H_5)] \xrightarrow{O_2} [Ru_2(CO)_4(\eta^5\text{-}C_5H_5)]_2 + H_2 \qquad \text{Eq. 2}$$

The complex **1** is stable to air and light in the solid state, but it decomposes in solution. Therefore it is important not to leave the solution standing for a long period of time in air, especially when performing column chromatography.

Compound **2**, $[Cp^*Ru(CO)_2]_2$, the analogue of (**1**) was obtained in high yield by the reaction of $Ru_3(CO)_{12}$ with six equiv. of pentamethylcyclopentadiene following the method described by King and Iqbal [43]. This complex was prepared in order to make a comparative study of its selectivity and activity with complex **1** in CO hydrogenation. Substituting H for CH_3 in the cyclopentadienyl ligand changes both the steric and electronic properties of the ligand. Unlike complex **1**, this compound is not very soluble but it is quite stable. Difficulty was experienced in purification of this compound and after several attempts to purify it by column chromatography, it was decided to omit this step. However, purification of this compound was achieved by extraction into CH_2Cl_2/ hexane (1:1). Recrystallisation by first dissolving the compound in CH_2Cl_2 and then adding a minimum amount of hexane after filtration afforded the product. Complex **2** is an orange crystalline compound, which decomposes at 280 °C (as observed in the Kofler hot-stage microscope).

Compound **3** was prepared by reacting (**1**) with MeLi in diethyl ether and the protonation of the resulting species leads to the formation of the complex [42].

Purification of the compound by column chromatography gave a yellow solid, which is stable in air and highly soluble. A yield of 32% was obtained.

2.3 Characterization of compounds 1, 2 and 3

As mentioned earlier, compounds **1**, **2** and **3** have been synthesized previously [42, 43]. The infrared data and the ^{1}H NMR data obtained for these complexes during the current study, compared well with the previously published data. Thus, the IR spectrum for complex **1** showed two ν(CO) absorption bands in CH_2Cl_2 at 2023 and 1938 cm^{-1}, which may be attributable to the *trans*-nonbridged isomer. The other two carbonyl bands at 1959 and 1770 cm^{-1} were assigned to the *trans*-bridged isomer, with the latter being due to the bridging CO. The weak band at 2004 cm^{-1} was due to the symmetric stretch of the *cis*-bridged isomer.

However, as expected, in the IR spectrum of complex **2**, two strong ν(CO) stretching bands at 1925 and 1744 cm^{-1} were observed in CH_2Cl_2. These bands are at lower frequencies than those observed for complex **1** and this is mainly due to the fact that Cp* is a better electron donor than Cp.

The IR spectrum of complex **3,** which was obtained as a mixture of *cis* and *trans*-isomers, showed a strong carbonyl band at 1974 cm^{-1} and two more medium bands at 1933 and 1776 cm^{-1}, with the latter being due to the bridging CO. The characterization data for all prepared compounds is summarised in Table 2.3.

Table 2.3: Characterization data for the ruthenium dimers.

Compd. No.	Yield (%)	M.p. (°C)	Infrared ν_{max} (CO)[a] (cm^{-1})
1	30	185-188	2023 s, 1959 s, 2004 w, 1938 sh, 1770 m
2	67	dec. 280	1925 s, 1744 s
3	32	228-230	1974 s, 1933 m, 1776 m

[a] Spectra recorded in CH_2Cl_2

Table 2.4: ^{1}H NMR data[a] for the complexes **1**, **2** and **3**

Compd. No.	C_5H_5	C_5Me_5	-CH	$-CH_3$
1	5.28 (s)	-	-	-
2	-	1.84(s)	-	-
3(*trans*)	5.18(s) 5.29(s)	-	3.04(d, 7Hz)[b]	10.97 (q, 7Hz)
3(*cis*)	5.18(s)	-	3.02(d, 7Hz)	10.97(q, 7Hz)

[a] Measured in $CDCl_3$ relative to TMS (δ = 0.00 ppm)

[b] *J* given in Hz

Table 2.4 gives the ^{1}H NMR data for complexes **1-3**. Complex **1**, gives a sharp singlet at δ = 5.28 ppm in the ^{1}H NMR for the η-C_5H_5 protons, which is fully consistent with its structure. In the ^{1}H NMR spectrum of complex **2** a sharp singlet at δ = 1.84 ppm is also observed for the η-C_5Me_5 protons. For complex **3**, the proton spectrum for the trans isomer shows a doublet at δ = 3.04 ppm (J = 7 Hz) due to the methyl protons, two singlets at δ = 5.18 ppm and 5.29 ppm for the C_5H_5 protons and quartet at δ = 10.97 ppm (J = 7 Hz) for the CH proton. The cis isomer shows a doublet at δ = 3.02 ppm (J = 7 Hz) for the methyl protons, a singlet at δ = 5.18 ppm for the two sets of C_5H_5 protons and a quartet at δ = 10.97 ppm (J = 7 Hz). The ^{1}H NMR spectra of complexes **1**, **2** and **3** are shown in Figures 2.5, 2.6 and 2.7, respectively.

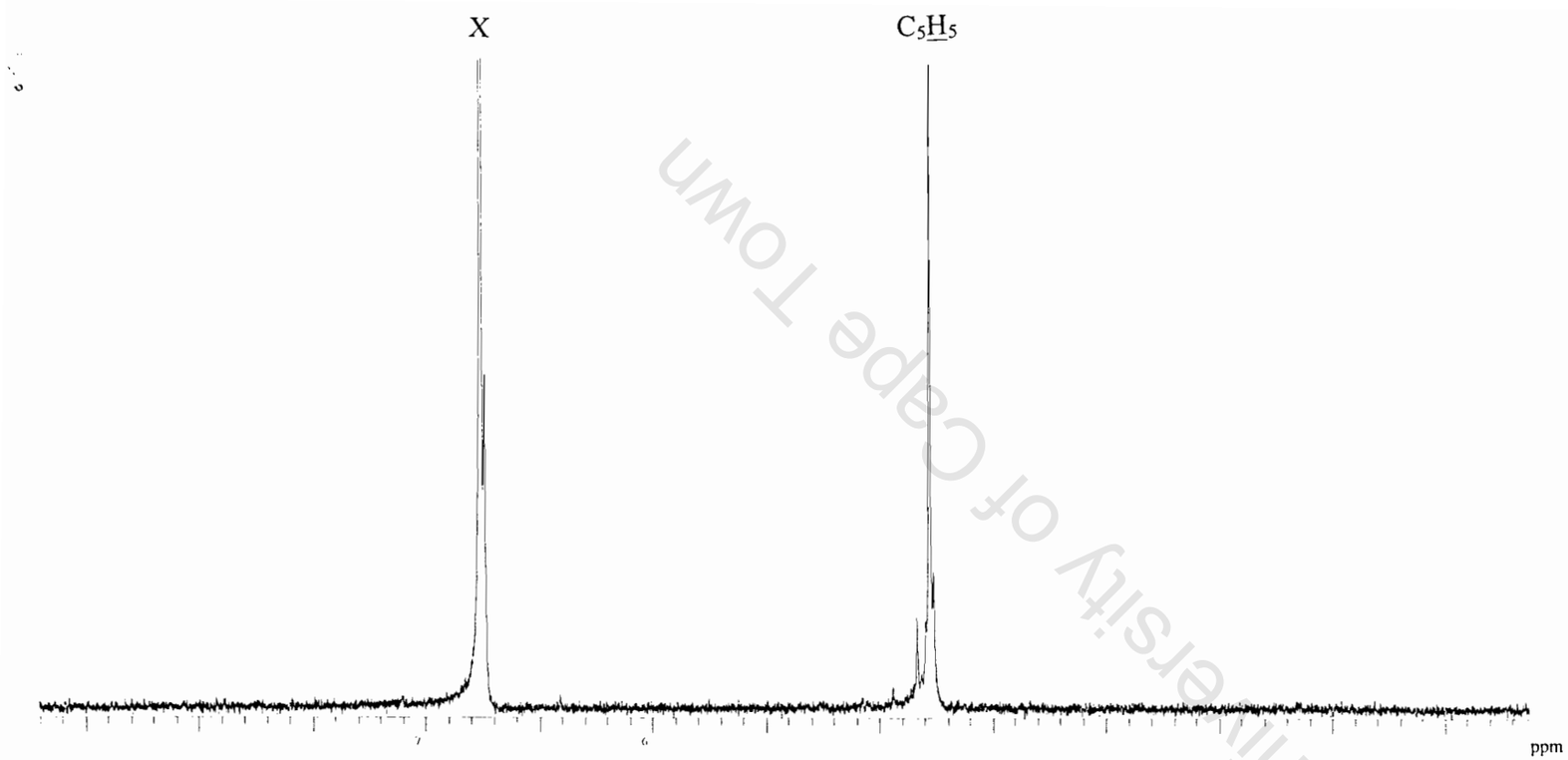

Figure 2.5: ^{1}H NMR spectrum of $[CpRu(CO)_2]_2$ (**1**) in $CDCl_3$ (X = solvent).

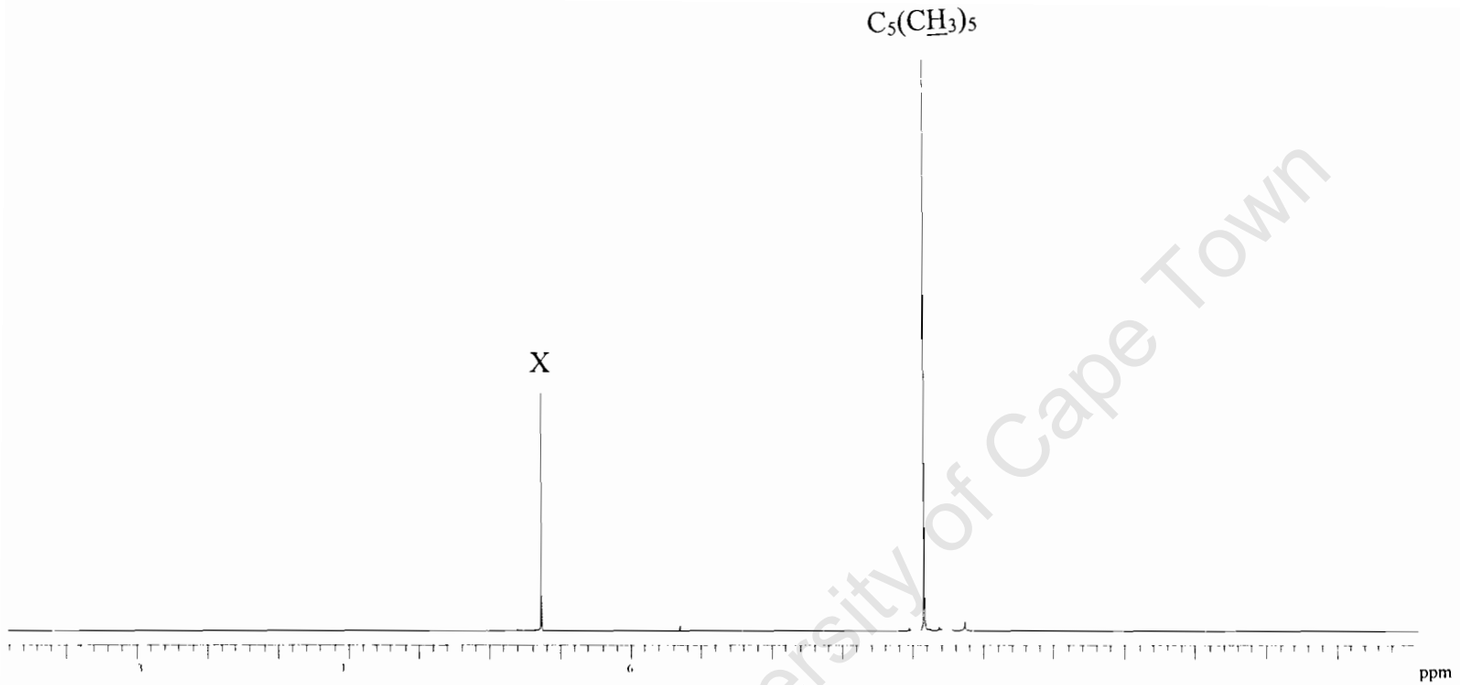

Figure 2.6: ^{1}H NMR spectrum of $[Cp^{*}Ru(CO)_2]_2$ (**2**) in $CDCl_3$ (X = solvent).

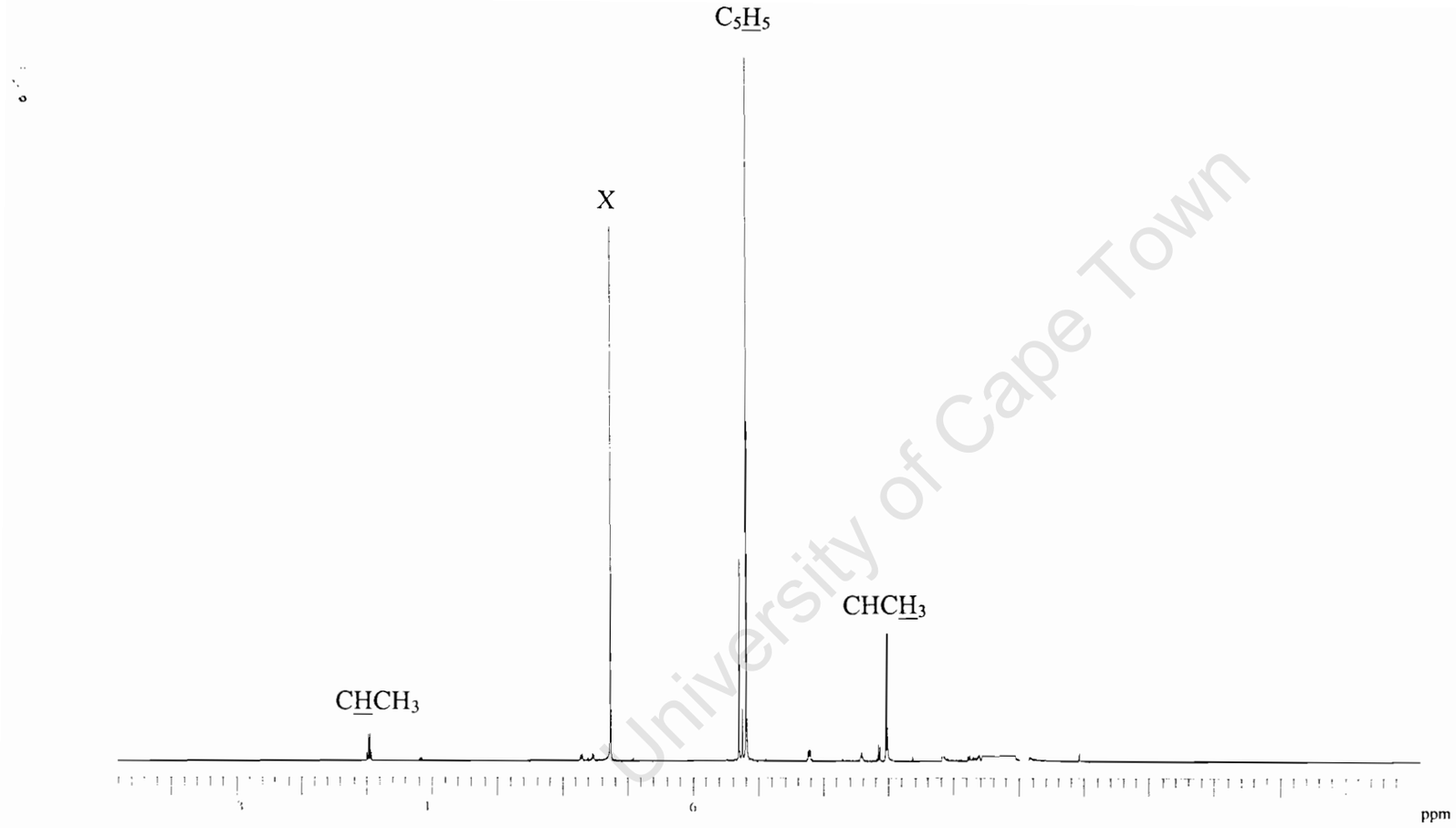

Figure 2.7: ^{1}H NMR spectrum of $[Ru_2(CO)_2(\mu\text{-}CO)(\mu\text{-}CHMe)(Cp)_2]$ (**3**) in $CDCl_3$ (X = solvent).

2.4 Catalytic CO hydrogenation reactions

Organometallic compounds are well known for their role in catalytic processes and great interest has developed in carbon monoxide hydrogenation reactions for either the synthesis of hydrocarbons, methanol or higher alcohols [15]. Metal carbonyl complexes are widely used as precursors to supported metal catalysts. The ruthenium carbonyl complexes were synthesized with the intention of using them as catalysts in CO hydrogenation reactions, which was specifically the focus of this work. Successful attempts have been made before to investigate the Fischer-Tropsch activity of the bi-nuclear $[CpRu(CO)_2]_2$ (**1**) and tri-nuclear $Ru_3(CO)_{12}$ complexes as well as the dendrimer supported on SiO_2, since it was previously found that a single metallic site is not sufficient for FT synthesis [44].

Of great interest would have been to investigate the FT activity of a dendrimer with dinuclear Ru-Ru units on the periphery (see Scheme 1), since previous studies have shown that the mono-atomic dendrimer is not active in Fischer-Tropsch synthesis. The synthesis of the dinuclear dendrimer was attempted, but unfortunately was not successful. However, a comparative study of the complex **1** with its pentamethyl analogue (**2**) was carried out. Complex **1** has been tested before by Claeys et al. and the results have been published [54]. This complex is less stable in H_2 containing atmospheres. In addition, complex **3**, which has also never been investigated before, was used to find out if substituting one of the bridging carbonyl ligands will make a noticeable difference in FT activity and product selectivity.

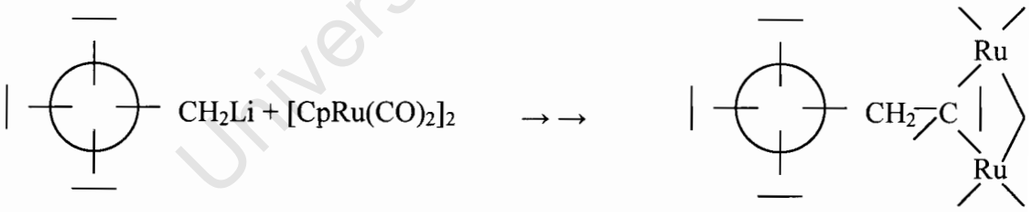

Scheme 1: Representation of the formation of the dendrimer with dinuclear Ru-Ru units.

2.4.1 Catalyst preparation and characterization

For comparison purposes, a standard Ru/SiO_2 catalyst was prepared by incipient wetness impregnation of SiO_2 (3wt % Ru loading) with an aqueous solution of $RuCl_3 \cdot 2H_2O$, as explained in Chapter 4. The solvent was removed at room temperature under flowing N_2 and the dried catalyst was pretreated in the FT synthesis U-tube reactor. The catalysts based on Ru complexes were prepared by impregnation onto SiO_2 using incipient wetness impregnation technique in acetone, ensuring 3wt % Ru loading, but unlike the standard catalyst, no further pretreatment was done.

Using the standard catalyst (0.4 g), FT synthesis was performed at 170 °C, pressure of 2 bar, H_2/CO ratio of 2:1 and v_{syngas} = 9ml(NTP)/min. The samples of the product stream were taken over a 24- hour period, initially at 20s intervals and then the intervals were increased gradually as the reaction progressed. About fifty samples were collected in ampoules using the ampoule sampling technique (see Chapter 4). In contrast, the complexes **1-3** are not stable on SiO_2 at temperatures above 170 °C and as a result they tend to decompose quickly, therefore samples are only taken for not more than 4 hours. Analysis of the samples was carried out using a gas chromatograph. The first peak in the GC trace is the methane peak, followed by C_2-, C_3-hydrocarbons and so on. The rate of formation, r is calculated (Eq. 1) using the peak areas, A_i.

$$r_i = (A_i / N_i) / (A_{CHx} / N_{CHx}) \cdot n_{ref,\,CHx} / m_{Ru} \qquad \text{Eq. 1}$$

where: n_{CHx} = molar flow rate of standard cyclohexane fed to the exhaust gas

CH_x = cyclohexane in the reference gas

A_i = peak area of each species

N_i = carbon number of each component

and

$$n_{ref,CHx} = X_{CHx(in\ ref)} \cdot V_{ref} / V_A \qquad (V_{ref} = 3 \text{ ml (NTP)/min})$$

$(X_{CHx} = 0.15\%$ cyclohexane in nitrogen)

2.4.2 CO hydrogenation with the standard Ru/SiO_2 catalyst

A plot of the rates of formation of C_1-C_3 compounds as a function of time on stream is shown below in Figure 2.8. The catalyst deactivates with time on stream before reaching steady state. The amount of methane (C_1) is higher than the amount of C_3 hydrocarbons, which is in turn higher than the amount of C_2 hydrocarbons.

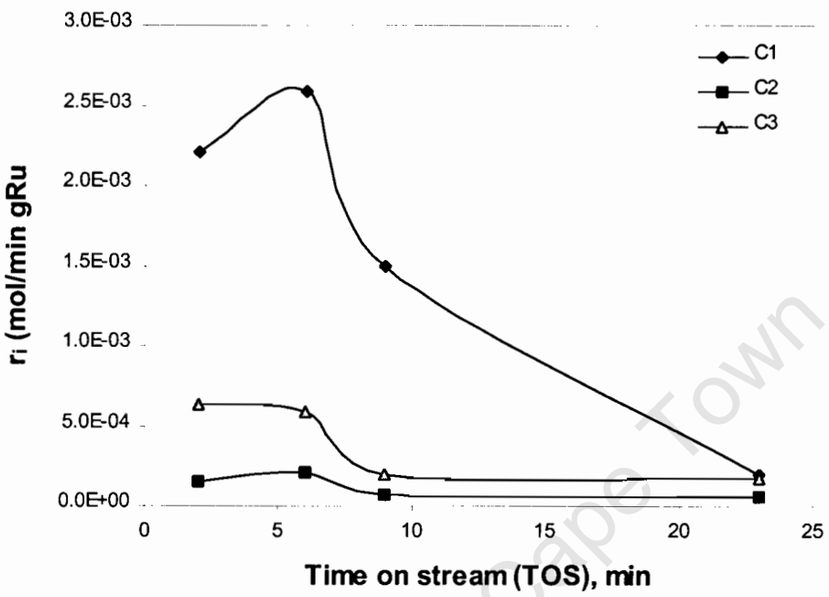

Figure 2.8: Formation rates of C_1-C_3 hydrocarbons for the standard Ru/SiO_2 catalyst.

Figure 2.9 shows an Anderson-Schulz-Flory (ASF) plot (logarithmic plot of molar product contents as a function of carbon number), which illustrates the formation of the hydrocarbon chain as one carbon unit is added at a time. A sharp kink at C_2 is observed which may be due to the re-adsorption of ethene, since it tends to undergo secondary reactions such as incorporation into growing chains resulting in lower quantities when compared to other hydrocarbons [29]. From the C_4 to C_7 hydrocarbon products, the slope of the line represents the chain growth probability, α. The calculated values for chain growth probabilities at different reaction times (ie 2 min, 5 min and 23 h) are 0.68, 0.42 and 0.56. These are quite similar to the values

obtained from the CO hydrogenation reaction of the standard Ru/SiO_2 catalyst by Claeys et al [44].

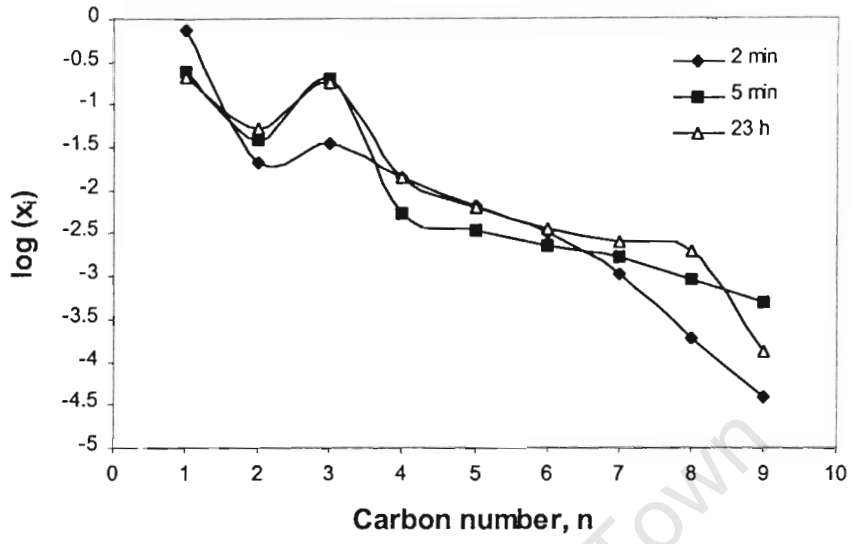

Figure 2.9: Anderson-Schulz-Flory (ASF) distribution for the standard Ru/SiO_2 catalyst.

Figure 2.10 shows a gas chromatogram (FID), which illustrates the product distribution obtained in the CO hydrogenation with the standard Ru/SiO_2 catalyst. Linear paraffins and olefins are the main products of FT synthesis.

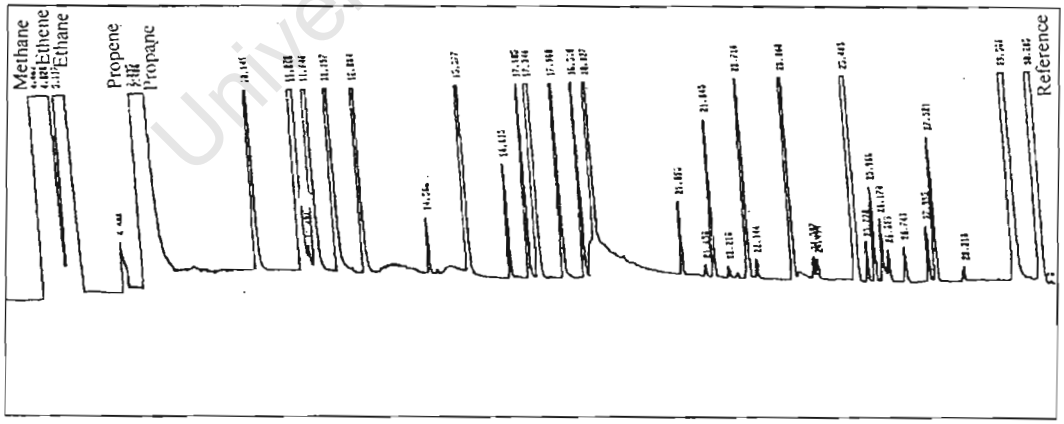

Figure 2.10: Gas chromatogram of the standard Ru/SiO_2 catalyst after 2 min TOS.

2.4.3 CO hydrogenation with $[CpRu(CO)_2]_2/SiO_2$

Figure 2.11 shows the formation rates of C_1-, C_2- and C_3-hydrocarbons obtained with $[CpRu(CO)_2]_2/SiO_2$. As with the standard catalyst, the rate of formation of methane is higher than the formation rates of C_2- and C_3-hydrocarbons. However, it was noticed with the standard catalyst that the formation rate of C_3 hydrocarbons is higher than that of C_2 hydrocarbons but the opposite was noticed with the dimer. In this case, the formation rate of C_3 hydrocarbons is lower than that of C_2 hydrocarbons. The presence of these compounds, however, indicates that there is indeed FT activity occurring.

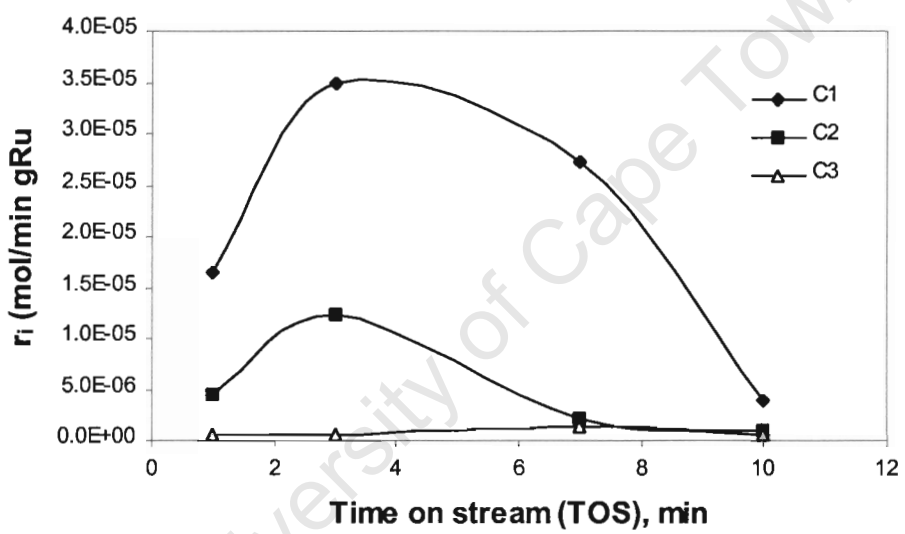

Figure 2.11: Formation rates of C_1-C_3 hydrocarbons for $[CpRu(CO)_2]_2/SiO_2$.

In FT synthesis, the syngas (H_2 + CO) with a ratio of 2:1 is fed into the system and the carbon monoxide is the primary source of carbon. However, in the case of the $[CpRu(CO)_2]_2$ catalyst it may be assumed that the carbonyl ligands are an alternative source of carbon. This was shown previously by feeding H_2 only [54].

The ASF plot for the experiment with the complex is shown below in Figure 2.12. It is quite clear that molar contents decrease linearly with an increase in carbon number. The chain growth probabilities, determined for C_1-C_3 at the different TOS (3 min, 7 min and 10 min) were found to be 0.15, 0.19 and 0.16. In comparison to the α values

obtained with the standard catalyst, the α values for this catalyst are quite low, which might be an indication of the occurrence of only primary reactions.

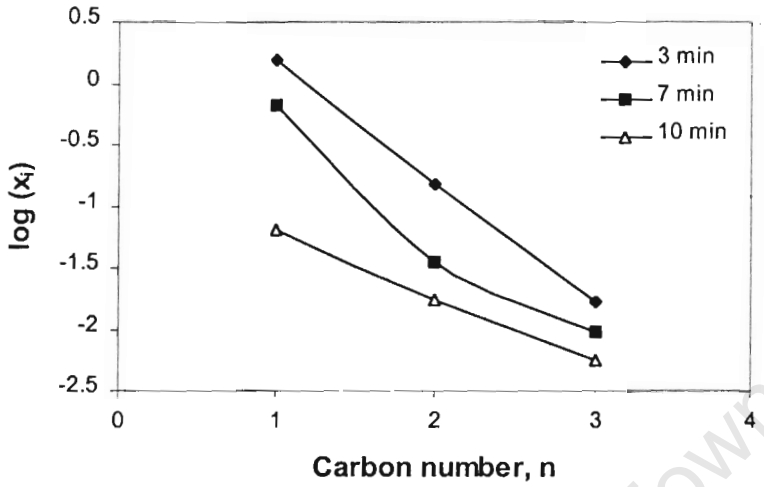

Figure 2.12: ASF distribution plot using $[CpRu(CO)_2]_2/SiO_2$ at three TOS.

A gas chromatogram (FID) obtained after 2 minutes using $[CpRu(CO)_2]_2$ is shown in Figure 2.13. Methane always comes out as the first peak and the peak next to it is the ethene peak, which is quite large when compared to the ethane peak following it, as expected. Propene is seen at 6.609 min, followed by propane, but they are quite small. The Cp ligand is observed as a broad peak at 14.670 min. The catalyst deactivates at higher TOS, which subsequently results in decrease in the rate of formation of C_1-C_3 hydrocarbons.

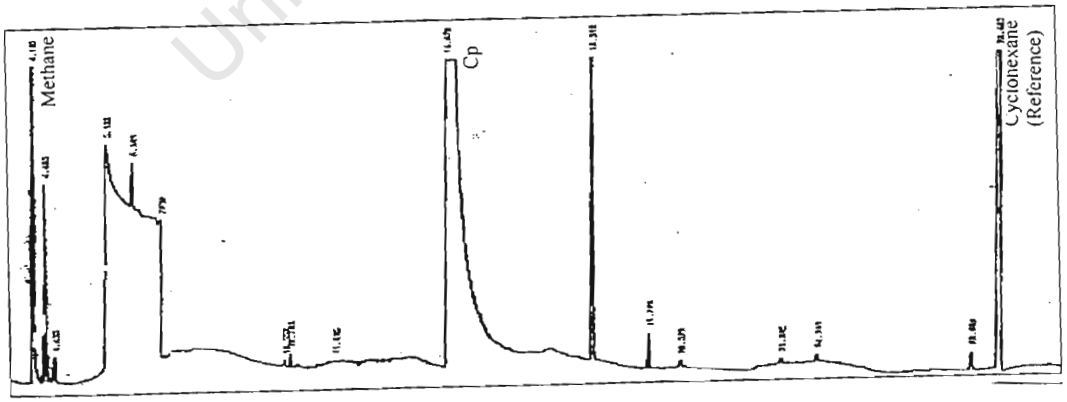

Figure 2.13: Gas chromatogram showing FT products of $[CpRu(CO)_2]_2/SiO_2$ after 2 min TOS.

2.4.4 CO hydrogenation with $[Cp^*Ru(CO)_2]_2/SiO_2$

The rate of formation of C_2- and C_3-hydrocarbons (see Figure 2.14) follows the same trend for the $[Cp^*Ru(CO)_2]_2$ and the $[CpRu(CO)_2]_2$ complex, whereby the C_2 hydrocarbons are in greater abundance than the C_3 hydrocarbons. This implies that substitution of the hydrogen in the Cp ligand with the methyl group appears to have little effect in FT activity and selectivity for these complexes. A similar deactivation pattern is also noticed.

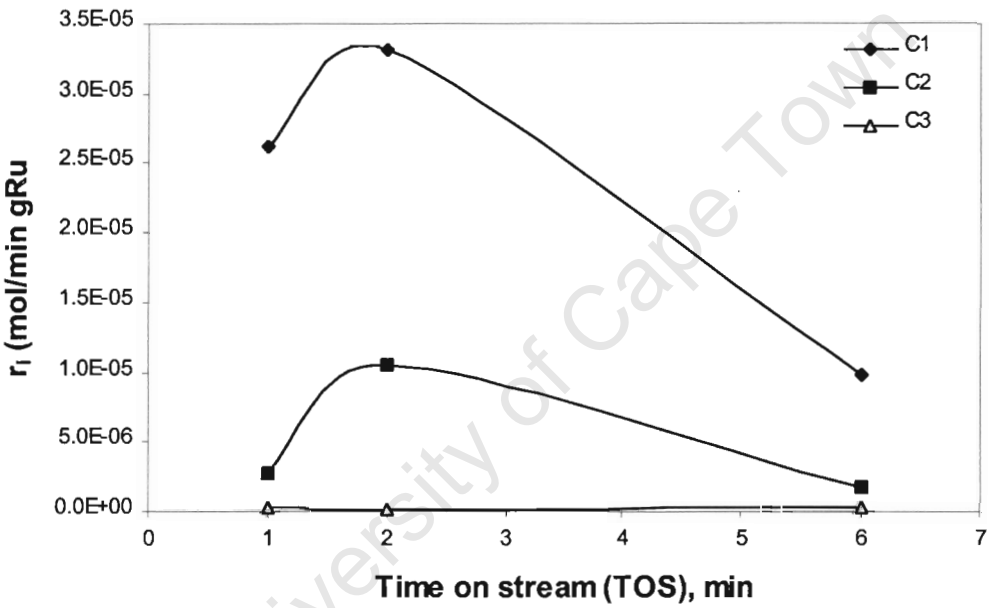

Figure 2.14: Formation rates of C_1-C_3 hydrocarbons for $[Cp^*Ru(CO)_2]_2/SiO_2$.

The chain growth probabilities for the $[Cp^*Ru(CO)_2]_2/SiO_2$ complex at the indicated times in the ASF plots (Figure 2.15), were found to be within the range 0.065 to 0.17. These values are significantly lower than those obtained for FT synthesis on the analogous complex $[CpRu(CO)_2]_2/SiO_2$, which suggests that by altering the ligand it is possible to influence the chain growth probability. These values indicate the independence of chain growth probability on time on stream and they also imply that no long chain hydrocarbons are being formed.

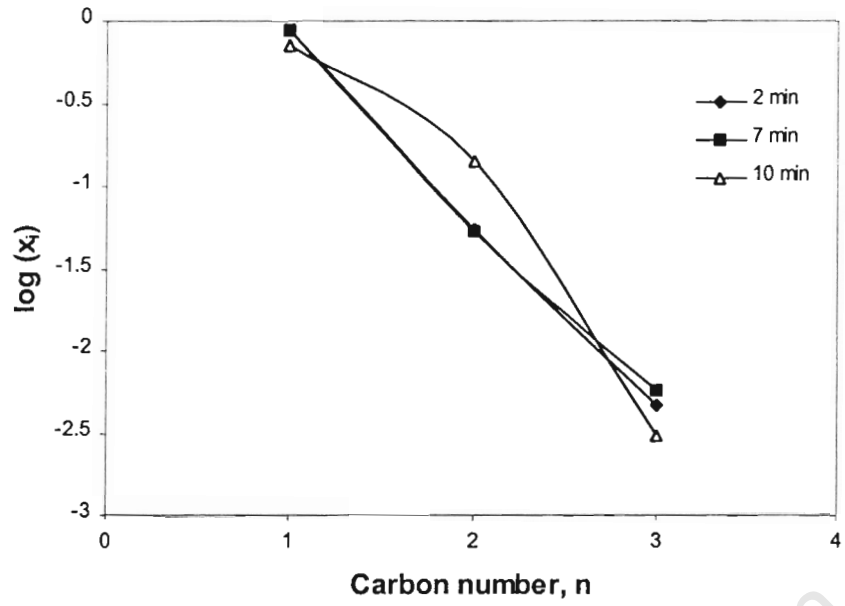

Figure 2.15: ASF distribution plot using $[Cp^*Ru(CO)_2]_2/SiO_2$ at three TOS.

The gas chromatogram (FID) in Figure 2.16 obtained after 2 minutes TOS shows a similar FT product pattern as observed with the complex $[CpRu(CO)_2]_2/SiO_2$ (Figure 2.13). The presence of the C_2 and C_3 hydrocarbons verifies that chain growth has taken place.

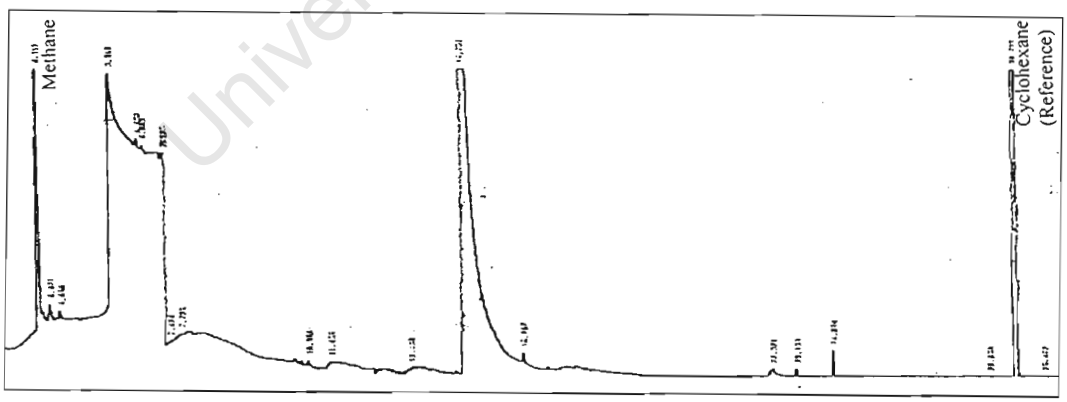

Figure 2.16: Gas chromatogram for FTS on $[Cp^*Ru(CO)_2]_2/SiO$ obtained after 2 min TOS.

2.4.5 CO hydrogenation with $[Ru_2(CO)_2(\mu\text{-}CO)(\mu\text{-}CHMe)(\eta^5\text{-}C_5H_5)_2]/SiO_2$

The complex $[Ru_2(CO)_2(\mu\text{-}CO)(\mu\text{-}CHMe)(\eta^5\text{-}C_5H_5)_2]/SiO_2$ behaved in a very interesting manner in terms of FT selectivity and also its stability. In addition to the formation of C_3-hydrocarbons, which indicate FT activity, also C_4- and C_5-hydrocarbons were observed, as shown below in Figure 2.17 in the chromatogram obtained after 2 minutes TOS. It is believed that the major source of C_2 hydrocarbons could be CHMe, which acts as a chain starter, meaning it is less likely that the C_2 hydrocarbons observed in Figure 2.17 are FT products. However, it is interesting to note that the slope in the ASF diagram (Figure 2.19) in the range C_1-C_2 seems to be the same as for the other complexes. This might indicate that CHMe is not consumed. The other two previous complexes deactivate after about 10 minutes TOS but, on the contrary, this complex was still stable after 1 hour TOS. Thus, changing the bridging ligand in the dimer seems to have an effect.

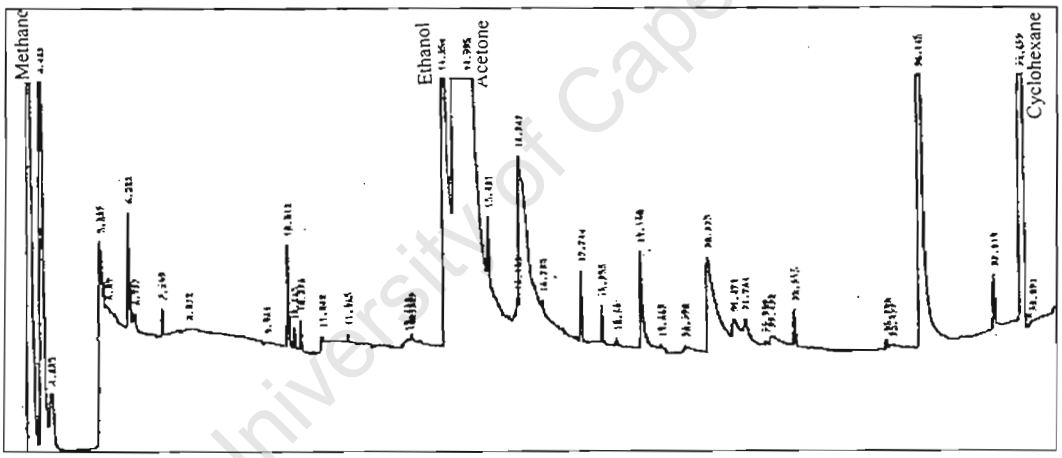

Figure 2.17: Gas chromatogram showing FT products obtained after 2 min TOS using $[Ru_2(CO)_2(\mu\text{-}CO)(\mu\text{-}CHMe)(\eta^5\text{-}C_5H_5)_2]/SiO_2$.

The product formation rates decrease with increasing TOS (see Figure 2.18). The maximum product formation with this complex is reached after 2 minutes TOS, however, it continues even up to 60 minutes.

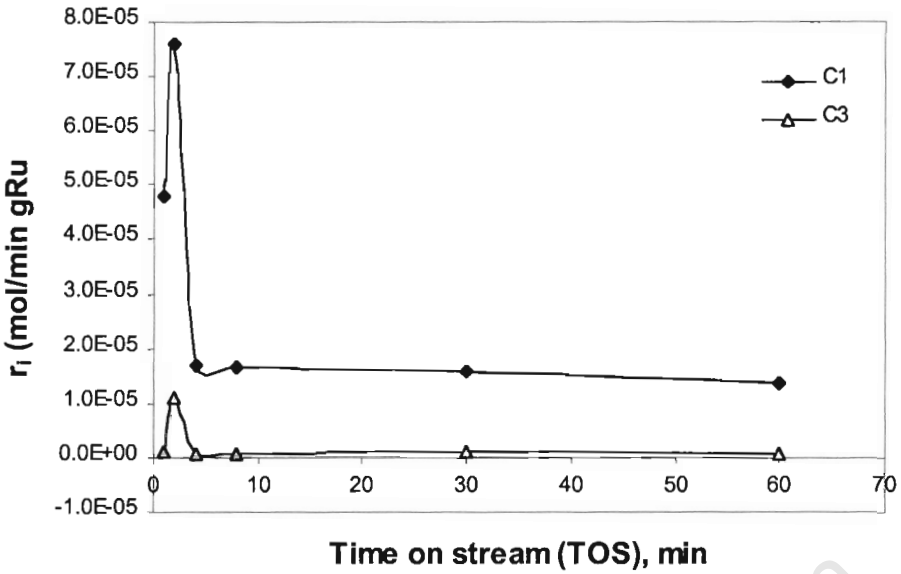

Figure 2.18: Rates of formation of C_1-and C_3- hydrocarbons during FT synthesis with $[Ru_2(CO)_2(\mu\text{-}CO)(\mu\text{-}CHMe)(\eta^5\text{-}C_5H_5)_2]/SiO_2$ over TOS.

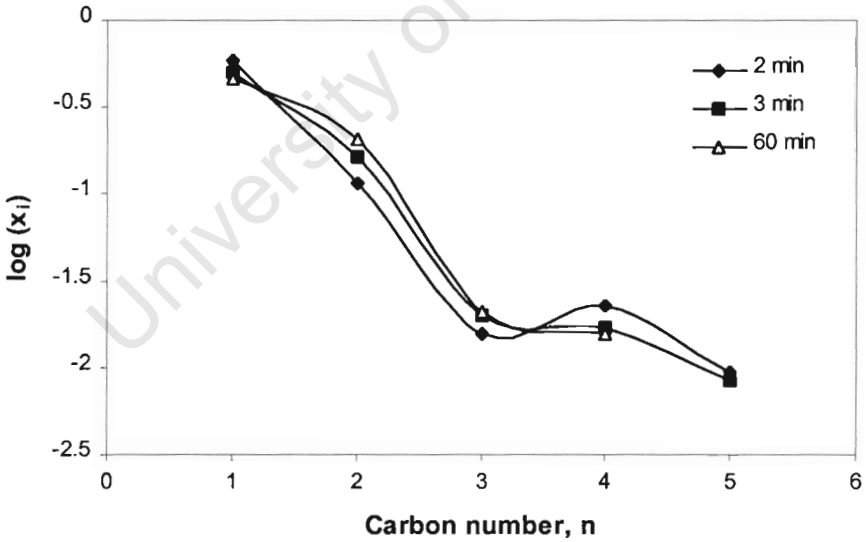

Figure 2.19: ASF distribution plot using $[Ru_2(CO)_2(\mu\text{-}CO)(\mu CHMe)(\eta^5C_5H_5)_2]/SiO_2$ at three TOS.

The confirmation of existence of polymerisation kinetics [47] is once again shown in the ASF plot (Figure 2.19), a trend observed with all the other syntheses. The

calculated values for chain growth probabilities (range C_3-C_5) for this complex were within the range 0.16 to 0.21. These values are slightly larger than those obtained using the other two complexes.

2.4.6 Olefin to paraffin ratios of the C_2- and C_3- fraction

The relative olefin to paraffin ratios of the C_2- and C_3- hydrocarbon fractions is shown in Table 2.4. For the standard Ru/SiO_2 the C_3 fraction is higher than the C_2 fraction and the opposite is observed for the other complexes.

Table 2.4: Olefin : paraffin ratios

Complex	C_2-fraction	C_3-fraction
Standard Ru/SiO_2	1.15	2.98
$[CpRu(CO)_2]_2/SiO_2$	2.49	1.96
$[Cp^*Ru(CO)_2]_2/SiO_2$	2.34	1.92
$[Ru_2(CO)_2(\mu\text{-}CO)(\mu\text{-}CHMe)(\eta^5\text{-}C_5H_5)_2]/SiO_2$	-	1.87

2.5 Conclusions

The complexes $[CpRu(CO)_2]_2$, $[Cp^*Ru(CO)_2]_2$ and $[Ru_2(CO)_2(\mu\text{-}CO)(\mu\text{-}CHMe)(\eta^5C_5H_5)_2]$ were successfully synthesized and characterized. All complexes proved to be effective precursors for Fischer-Tropsch synthesis. It was shown that the substitution of the hydrogen atoms with methyl groups does not make a significant difference in the activity of FT reaction. However, the substitution of the bridging carbonyl group with –CHMe made a significant difference. Not only did the complex $[Ru_2(CO)_2(\mu\text{-}CO)(\mu\text{-}CHMe)(\eta^5C_5H_5)_2]/SiO_2$ show more FT activity, it was also more stable for a longer period of time when compared to the other two complexes.

Previous studies by Claeys et al. [54] have shown that more than one metallic site is needed for the Fischer-Tropsch synthesis and this work has supported the idea that two ruthenium atoms are required to catalyse the C-C bond formation.

CHAPTER 3

RESULTS AND DISCUSSION: EXPERIMENTS WITH OSMIUM

3.1 Introduction

The chemistry of osmium has been studied extensively with a high degree of interest shown in its tendency to form metal clusters [46]. Osmium, like ruthenium, is found in group VIII in the periodic table and these two metals tend to resemble each other in their lower oxidation state chemistry. Osmium is as rare as ruthenium and their high price limits their commercial application as heterogeneous catalysts [46]. The complex $[CpOs(CO)_2]_2$ (Figure 3.1), an analogue of the ruthenium complex $[CpRu(CO)_2]_2$, was synthesized and its activity in Fischer-Tropsch synthesis was investigated. The compound $(NH_4)_2OsCl_6/SiO_2$ was supported onto SiO_2 (3wt % Os) and was used as the standard catalyst, taking into consideration that osmium, when compared to ruthenium is heavier. In addition to these two compounds, a tri-atomic complex, $Os_3(CO)_{12}$, was also supported on SiO_2 and the catalyst was investigated and the results were compared to those obtained for the analogous ruthenium catalyst, which has been previously studied (see Chapter 2).

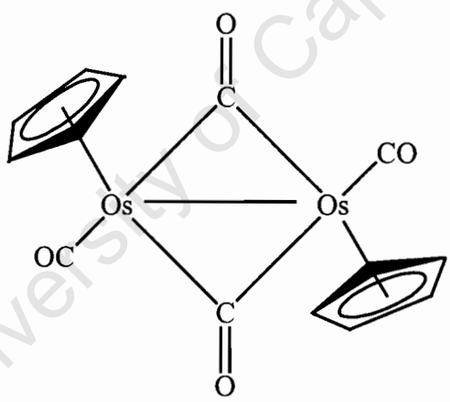

4

Figure 3.1: Depiction of a possible structure of the complex $[CpOs(CO)_2]_2$ (**4**).

3.2 Synthesis of $[CpOs(CO)_2]_2$ (4)

Complex **4** was synthesized from $(NH_4)_2OsCl_6$ in four steps, equations (1), (2), (3) and (4). The synthetic procedure for $[Os(CO)_3Cl_2]_2$ in the first step which is described in the work by Herrmann, Herdtweck and Schäfer [47] was not followed, instead a different method was used to prepare $[Os(CO)_3Cl_2]_2$. The reaction was carried out in a heated autoclave. Upon heating the mixture of $(NH_4)_2OsCl_6$ in ethanol, in flowing carbon monoxide, formation of $[Os(CO)_3Cl_2]_2$ in 59% yield occurs (Eq. (1)).

$$(NH_4)_2OsCl_6 \xrightarrow[175\ ^\circ C]{CO\ (70\ bar)} [Os(CO)_3Cl_2]_2 \qquad (1)$$

Reaction of $[Os(CO)_3Cl_2]_2$ with NaCp produced a hydride, $[CpOs(CO)_2H]$ (Eq. (2)) with a yield of 88% (lit. 77-92%).

$$[Os(CO)_3Cl_2]_2 + 2NaCp \xrightarrow[THF]{Room\ \ Temp.} [CpOs(CO)_2H] \qquad (2)$$

By utilizing the reaction sequence, in Eqs. (3) and (4), $[CpOs(CO)_2]_2$ (**4**) is obtained in 45% yield.

$$[CpOs(CO)_2H] + Ph_3CPF_6 \xrightarrow[THF]{Room\ Temp.} [CpOs(CO)_2]^+\ PF_6^- \qquad (3)$$

This important reaction whereby a hydride is abstracted from a transition metal was discovered by Beck and Schloter [48].

$$[CpOs(CO)_2]^+\ [PF_6]^- + [CpOs(CO)_2H] \xrightarrow[CH_2Cl_2]{N(C_2H_5)_3} [CpOs(CO)_2]_2 + [HN(C_2H_5)_3]^+\ PF_6^- \qquad (4)$$

The hydride reacts with a trityl cation, Ph_3CPF_6, to form $[CpOs(CO)_2]^+$ (Eq. (3)). The reaction of Eq. (4) is presumed to proceed by nucleophilic attack of the amine on the hydride resulting in a loss of the proton to give the nucleophile $[CpOs(CO)_2]^-$, which reacts with $[CpOs(CO)_2]^+$ to yield the dimer $[CpOs(CO)_2]_2$.

3.3 Characterization of $[CpOs(CO)_2]_2$ (4)

This complex was characterized by infrared spectroscopy, ^1H NMR spectroscopy and elemental analysis. These data have been previously reported [47]. The infrared spectrum with the solvent hexane shows two very strong ν(CO) absorption bands at 2020 and 1961 cm^{-1}. These bands are due to the hydride, $[CpOs(CO)_2H]$, which readily decomposes in Fischer-Tropsch synthesis to $[CpOs(CO)_2]_2$. The other two strong bands at 2041 and 1988 cm^{-1} are due to the terminal CO groups of the dimer, $[CpOs(CO)_2]_2$. In comparison, the IR spectrum of the ruthenium analogue of this compound $[CpRu(CO)_2]_2$ showed a band at 1770 cm^{-1}, which is due to the bridging CO groups but this was absent in the IR spectrum of compound **4**. This suggests that, unlike $[CpRu(CO)_2]_2$, the structure of compound **4** has terminal CO groups not bridging CO groups (see Figure 3.2).

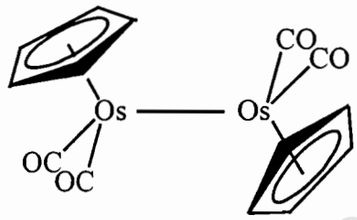

Figure 3.2: Structural representation of the trans isomer of $[CpOs(CO)_2]_2$

In the ^1H NMR spectrum of this complex, a singlet at δ = 4.86 ppm (lit. 4.82 ppm) for the η-C_5H_5 protons is observed. The ^1H NMR spectrum of complex **4** is shown in Figure 3.3.

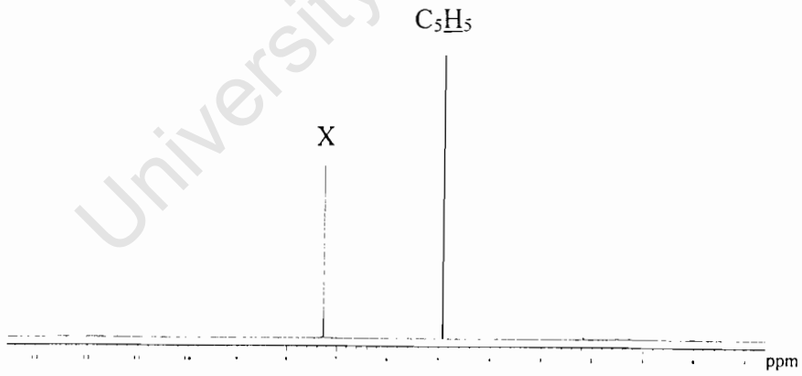

Figure 3.3: ^1H NMR spectrum of $[CpOs(CO)_2]_2$ (**4**) in $CDCl_3$ (X = solvent).

3.4 Catalytic CO hydrogenation reactions

It has been mentioned earlier that the catalysts that are active for the Fischer-Tropsch reaction are iron, cobalt, nickel and ruthenium. Studies have also shown that rhodium is also an active catalyst for the reaction but not much work has been done on osmium to investigate its activity in CO hydrogenation. As mentioned earlier, it appears from the work done by Choplin and Leconte [49] that $Os_3(CO)_{12}$ has a little FT activity. They carried out their experiments at 250 °C and a pressure of 1 bar. The H_2/CO ratio was 1:1. In this work, the H_2/CO ratio was kept at 2:1 since FT reactions are normally carried out at this ratio [2].

The experimental set-up used for the ruthenium experiments was also used for the osmium experiments, with the addition of a glass tube fitted in the exhaust gas line and with pieces of rubber and grease, which served as a " trap" for any osmium tetroxide, if it is formed. The Os-dimer, $[CpOs(CO)_2]_2$ was synthesized in order to compare its Fischer-Tropsch properties with those of the analogous Ru compound. The CO hydrogenation reactions have previously been done with the $Ru_3(CO)_{12}/SiO_2$ catalyst [44] and the results are compared in this work to those obtained with the $Os_3(CO)_{12}/SiO_2$ catalyst.

3.4.1 Catalyst preparation and characterization

The bi-and tri-nuclear complexes, $[CpOs(CO)_2]_2$ and $Os_3(CO)_{12}$, respectively, were impregnated on SiO_2 (3wt % Os loading) using incipient wetness impregnation method in acetone. The solvent was removed by blowing N_2 over the mixture at room temperature and no further pretreatment was done. For comparison purposes, a standard Os/SiO_2 catalyst was prepared by impregnation of SiO_2 with an aqueous $(NH_4)_2OsCl_6$ solution using incipient wetness method. The dried catalyst was pretreated in the FT synthesis reactor to remove chlorides by reduction in flowing H_2 at 4°C/min up to 300°C for 5 h.

3.4.2 CO hydrogenation with the standard Os/SiO_2 catalyst

Initially, the reaction temperature and pressure were set at 170 °C and 1 bar, respectively, since CO hydrogenation experiments on ruthenium were carried out under the same conditions. Almost no FT-activity was noticed at 170 °C, therefore the temperature was slowly increased to 200 °C and it slightly improved. There was even more improvement at temperatures 220 °C and 240 °C, the highest FT activity was observed at 300 °C.

Figure 3.4 shows the gas chromatograms (FID) at unchanged split ratios obtained at different temperatures (170, 200, 220, 240 and 300 °C) to illustrate the increase in activity of the standard Os/SiO_2 catalyst with increasing temperature.

(a)

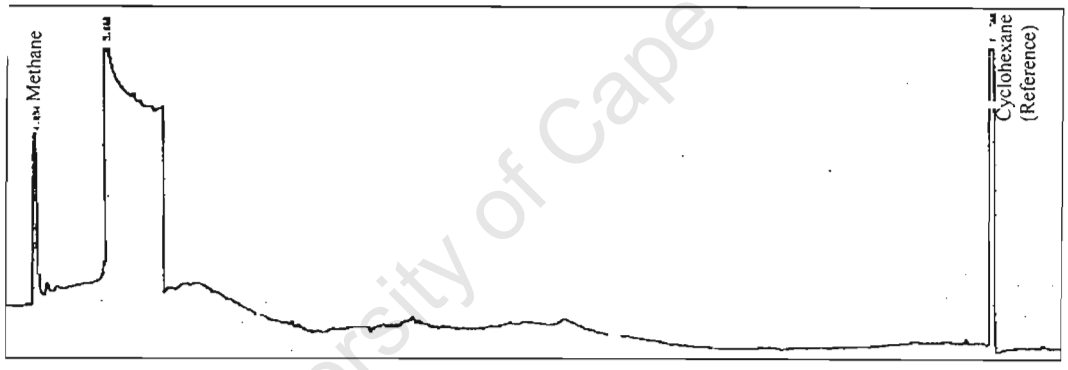

(b)

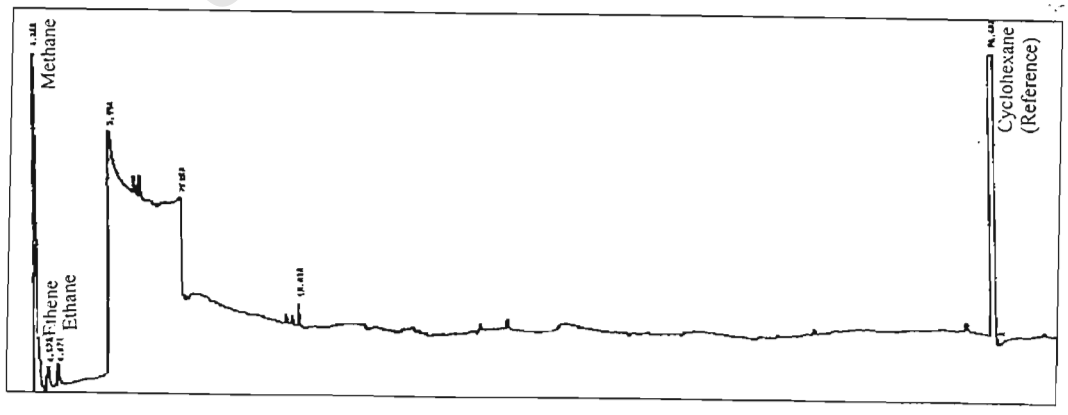

(c)

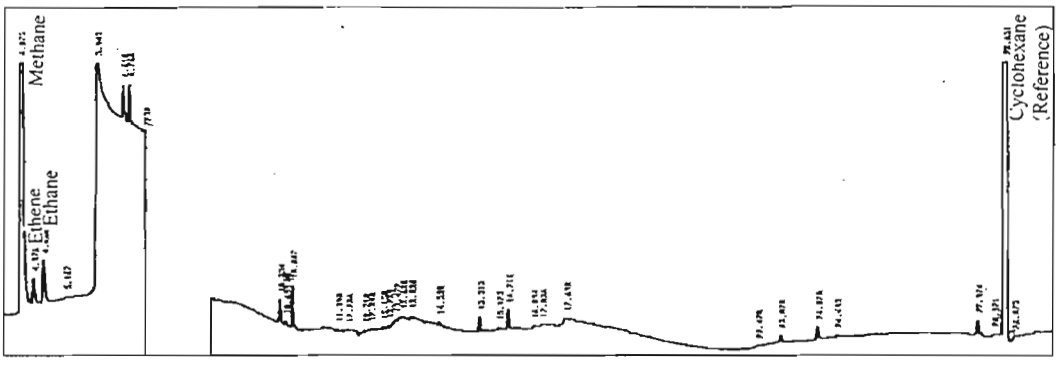

(d)

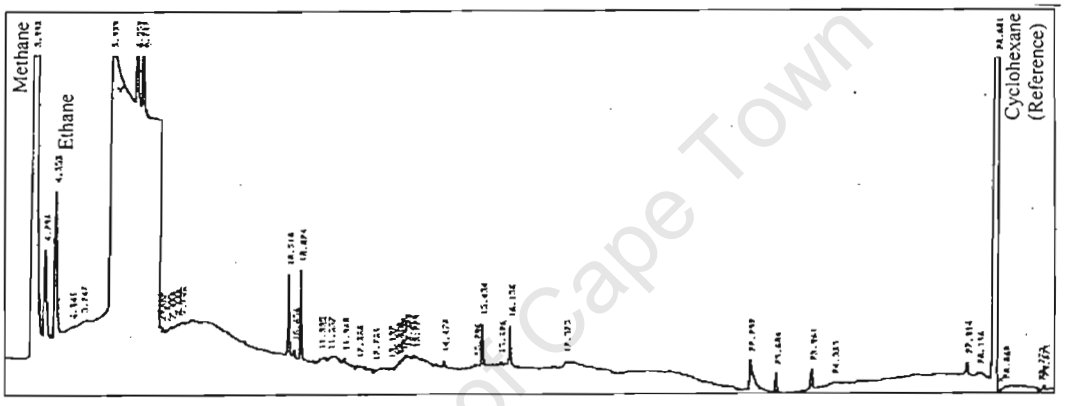

(e)

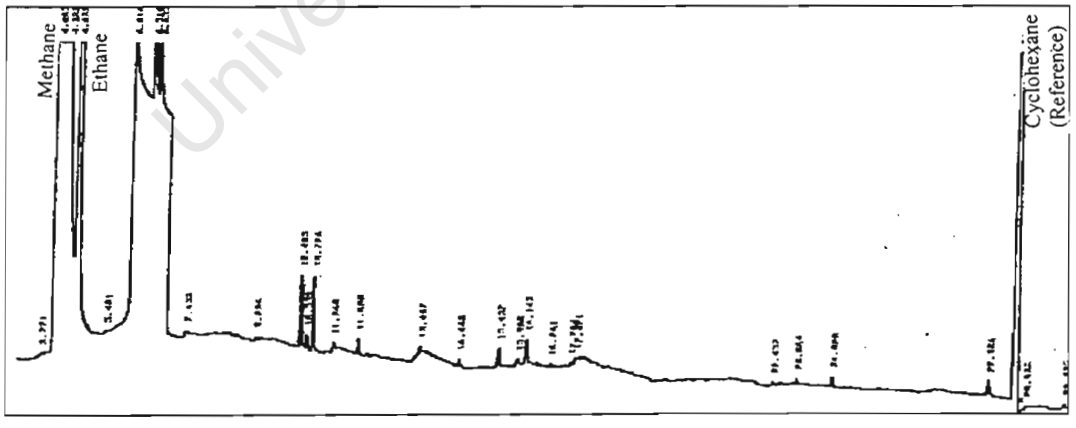

Figure 3.4: Comparison of five GC chromatograms using the standard Os/SiO_2 catalyst at:(a) 170 °C (no FT activity), (b) 200 °C, (c) 220 °C (d) 240 °C and (e) 300°C (highest FT activity).

Since less or no significant FT activity was observed at 170 °C and also taking into account the decomposition of the di- and tri-nuclear complexes at high temperatures, it seemed logical to perform the experiments on the complexes at both 170 and 220 °C. The two complexes $[CpOs(CO)_2]_2$ and $Os_3(CO)_{12}$ showed activity at 170 °C, thereby allowing comparison of the results with those obtained for the analogous Ru compounds at the same temperature. The results for the CO hydrogenation using the standard Os/SiO_2 catalyst were compared with those for the $[CpOs(CO)_2]_2/SiO_2$ and $Os_3(CO)_{12}/SiO_2$ catalysts at 220 °C.

Judging from the GC chromatogram of the standard Os/SiO_2 obtained after 4 minutes TOS (Figure 3.5) that osmium is not as active as ruthenium, probably due to the fact that the molar content of Os is only approximately half of that of Ru and, generally, osmium is not a good catalyst, but the fact that the C_2-, C_3- and C_4-hydrocarbons are formed indicates the occurrence of FT activity.

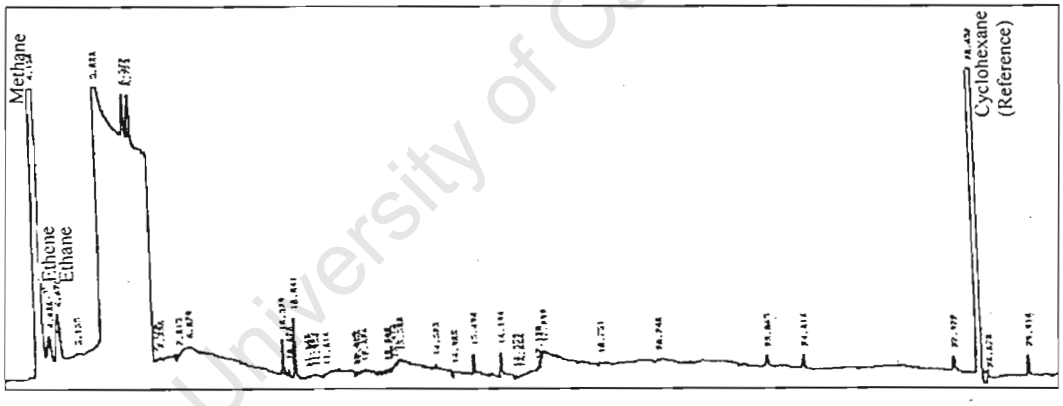

Figure 3.5: Gas chromatogram of the standard Os/SiO_2 catalyst after 4 min TOS at 220 °C.

Figure 3.6 shows the formation rates at three different reaction times. The rate of CH_4 formation dominates in comparison to the formation rates of the C_2- and C_3-hydrocarbons. As with the Ru standard catalyst, the yield of C_3- HC's is higher than the yield of C_2- HC's. Comparison of this plot of the rate of formation of the standard

Os/SiO_2 catalyst with the similar plot for the standard Ru/SiO_2 catalyst reveals that the pattern is fairly in good agreement.

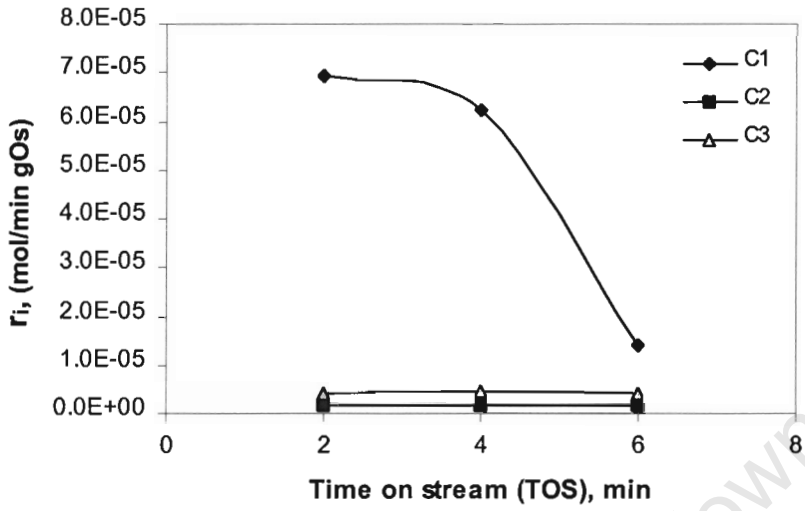

Figure 3.7: Rates of formation of volatile organic compounds during FT synthesis using the standard Os/SiO_2 catalyst at 220 °C.

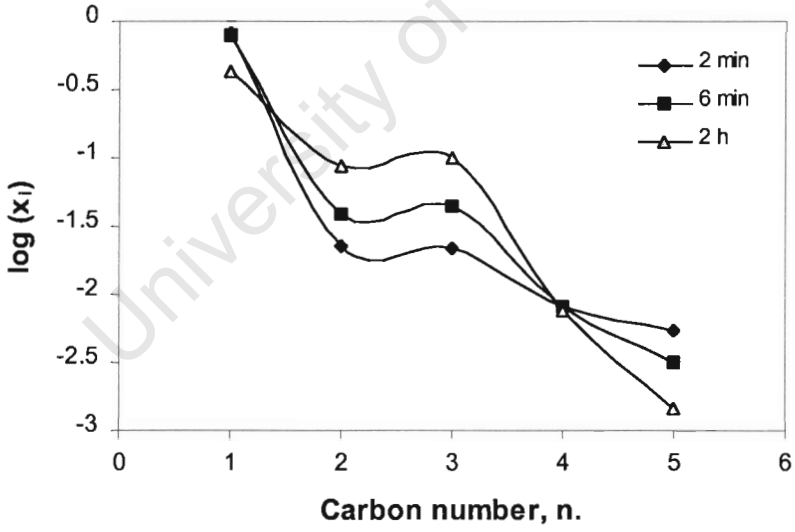

Figure 3.8: ASF distribution plot using the standard Os/SiO_2 catalyst at three TOS.

There is a slight discrepancy between the ASF plots of the standard Os/SiO_2 and Ru/SiO_2 catalysts. The sharp dip at C_2, which was observed with the Ru/SiO_2 catalyst, is less pronounced for the Os/SiO_2 catalyst, as shown in Figure 3.8, but apart from that, the decrease in the amount of hydrocarbons with an increasing carbon

number is noticed for both catalysts. The α values obtained using the base osmium catalyst are not very different from the ones which were obtained with the standard ruthenium catalyst. They were found to be 0.62, 0.43 and 0.28.

3.4.3 CO hydrogenation with the $[CpOs(CO)_2]_2/SiO_2$

The CO hydrogenation reactions using $[CpOs(CO)_2]_2/SiO_2$ were performed at two different temperatures, as mentioned earlier, and the reasons for doing that have already been discussed. Figure 3.9 is a representation of the results obtained at 170 and 220 °C and both chromatograms were obtained after 5 minutes TOS. The chromatogram at 170 °C matches the one obtained at the same temperature and TOS for $[CpRu(CO)_2]_2/SiO_2$ (Figure 2.13) and it is very clear that, on mass/molar basis, the ruthenium catalyst is more active than the osmium catalyst.

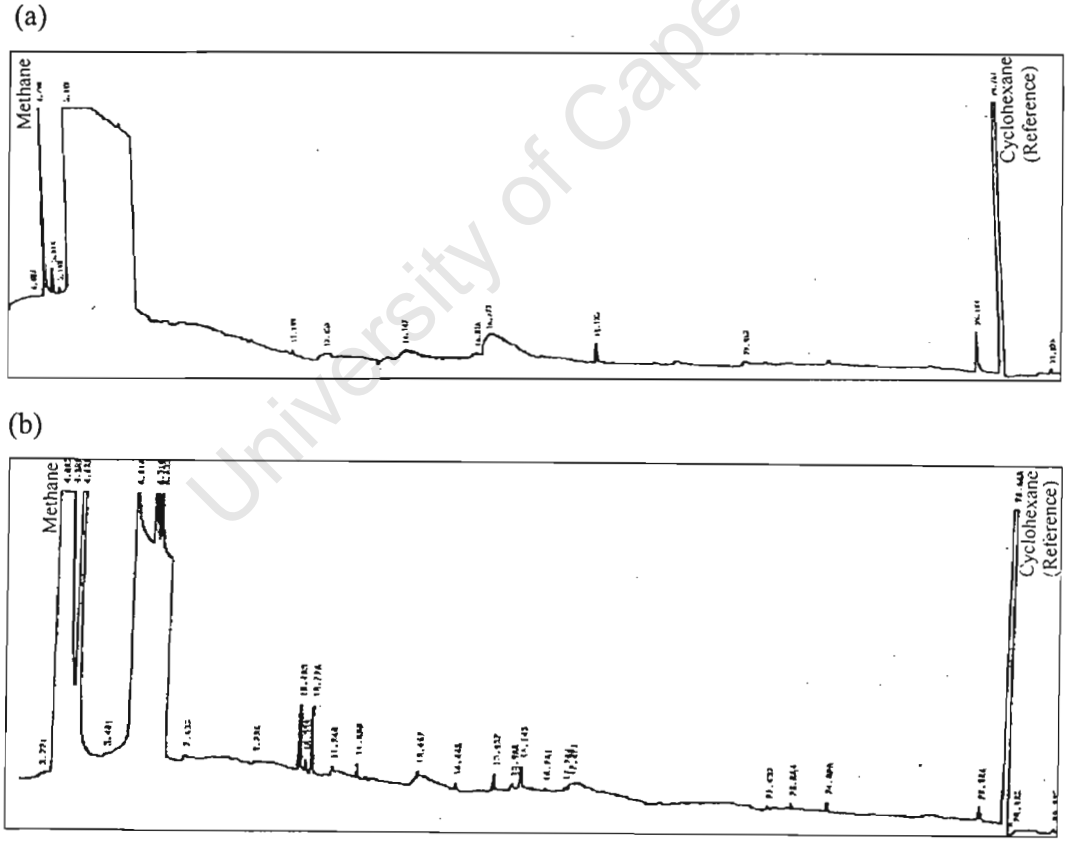

Figure 3.9: Comparison of two gas chromatograms obtained using $[CpOs(CO)_2]_2/SiO_2$ at: (a) 170 °C and (b) 220 °C

Figure 3.10 compares the formation rates of C_1-, C_2- and C_3-hydrocarbons for the CO hydrogenation experiments at 170 and 220 °C. At both temperatures the yield of methane is higher than the other two hydrocarbons, a similar trend noticed for the analogous ruthenium catalyst.

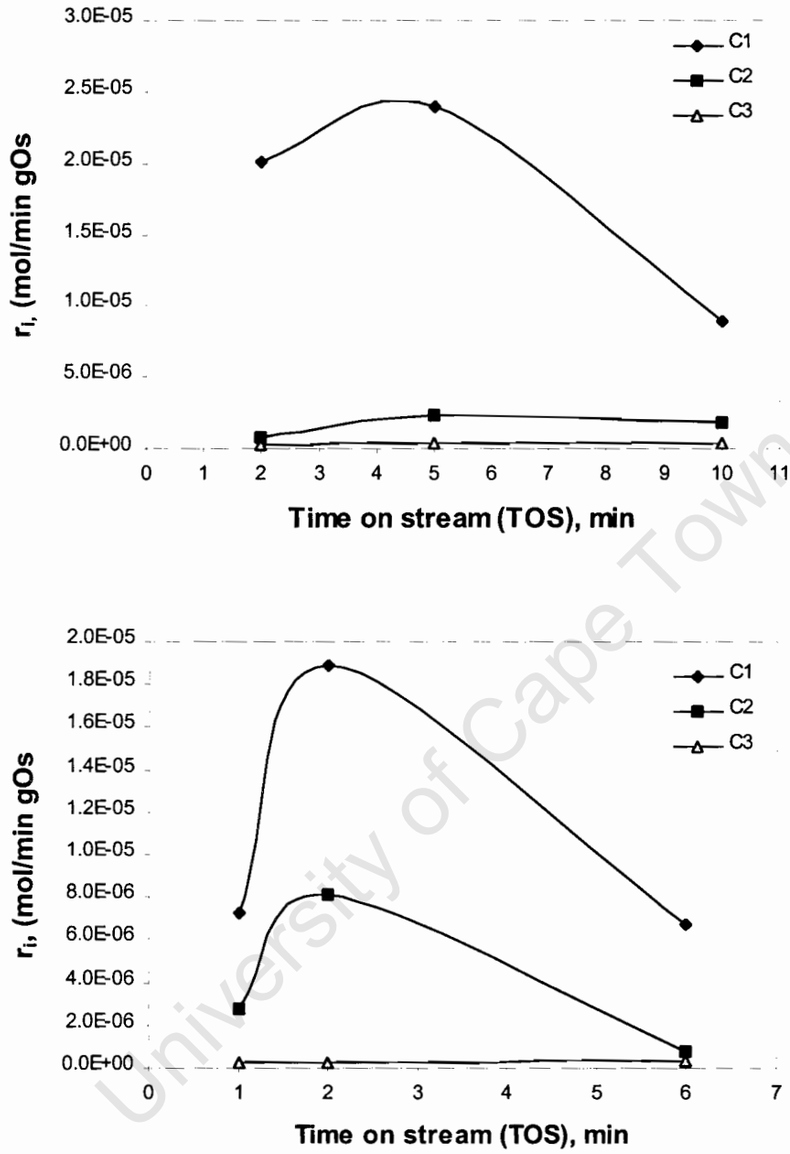

Figure 3.10: Formation rates using $[CpOs(CO)_2]_2/SiO_2$ at top: 170 °C and bottom: 220 °C.

The ASF distribution plots are shown in Figure 3.11 for the CO hydrogenation using $[CpOs(CO)_2]_2/SiO_2$. A similar trend is observed at both temperatures and, in addition, when compared to the FT synthesis with the analogous ruthenium complex there is not much difference either. The chain growth probability values obtained for this synthesis at 170 °C at the given reaction times (2 min, 5 min and 10 min) are ranging from 0.12 to 0.39. In contrast, at 220 °C the α values obtained at different reaction times (1 min, 6 min and 10 min) are within the range 0.075 to 0.083 for $[CpOs(CO)_2]_2/SiO_2$.

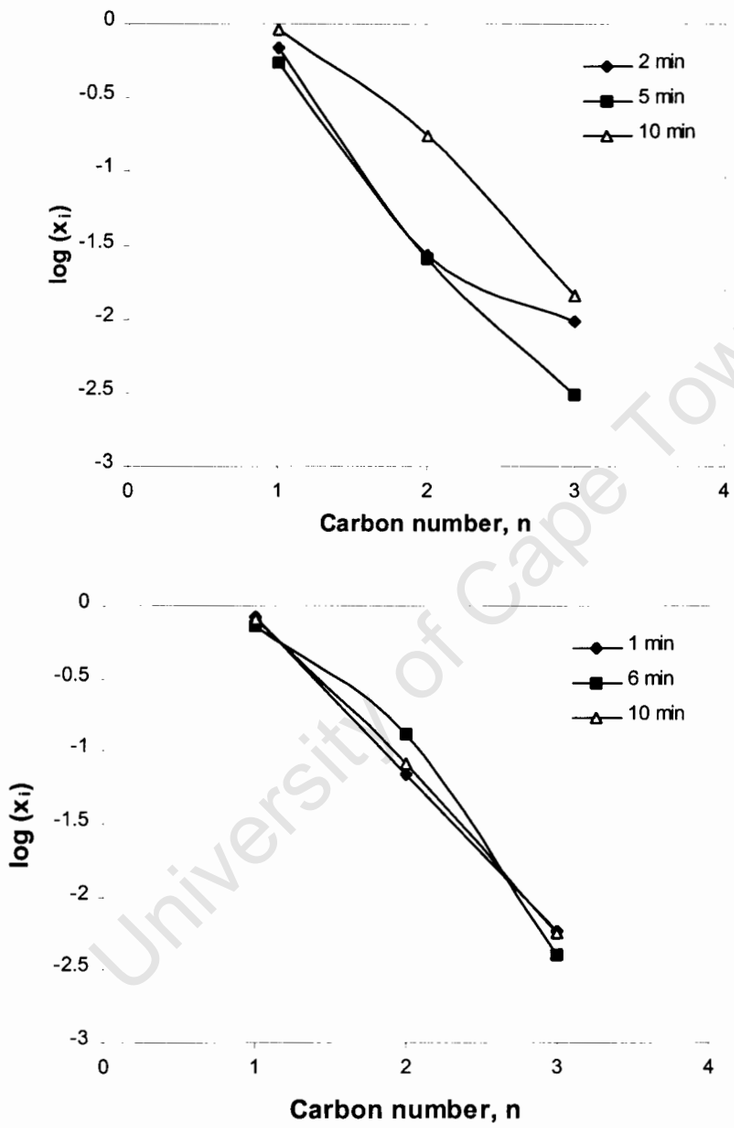

Figure 3.11: ASF distribution using $[CpOs(CO)_2]_2/SiO_2$ at top:170 °C and bottom: 220 °C.

3.4.4 CO hydrogenation with $Os_3(CO)_{12}/SiO_2$

The formation rates at reaction temperatures of 170 and 220 °C are shown in Figure 3.12. Only one FID measurement was obtained at 170 °C after 2 minutes TOS due to unavailability of the GC. The yield of methane is higher than the yield of C_2-and C_3-hydrocarbons. It is also noticed that the rate of formation of methane is much higher than that of the standard Ru/SiO_2 at the same temperature. This cannot be explained because it was expected that osmium is less active than ruthenium. At 220°C, in particular, the rate of formation of methane reaches a maximum after seven minutes TOS and then it declines rapidly. It is shown that the rate of formation of C_2 hydrocarbons is higher than the rate of formation of C_3 hydrocarbons.

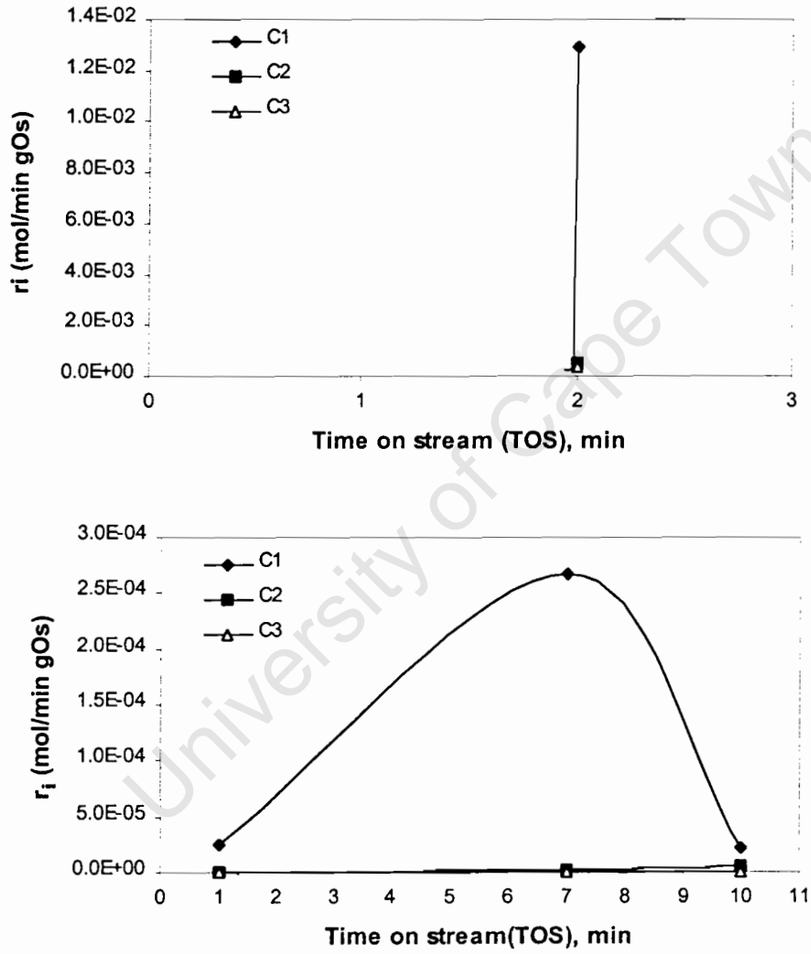

Figure 3.12: Comparison of the formation rates using $Os_3(CO)_{12}/SiO_2$ at top: 170 °C and bottom: 220 °C.

A similar study was done previously with the analogous ruthenium complex and the results showed that the complex deactivates after about 2 minutes TOS. In comparison, the results of this current study show that $Os_3(CO)_{12}/SiO_2$ deactivates after about 7 minutes TOS at 220°C. This could possibly mean that the osmium complex is more stable than its ruthenium analogue, as would be expected.

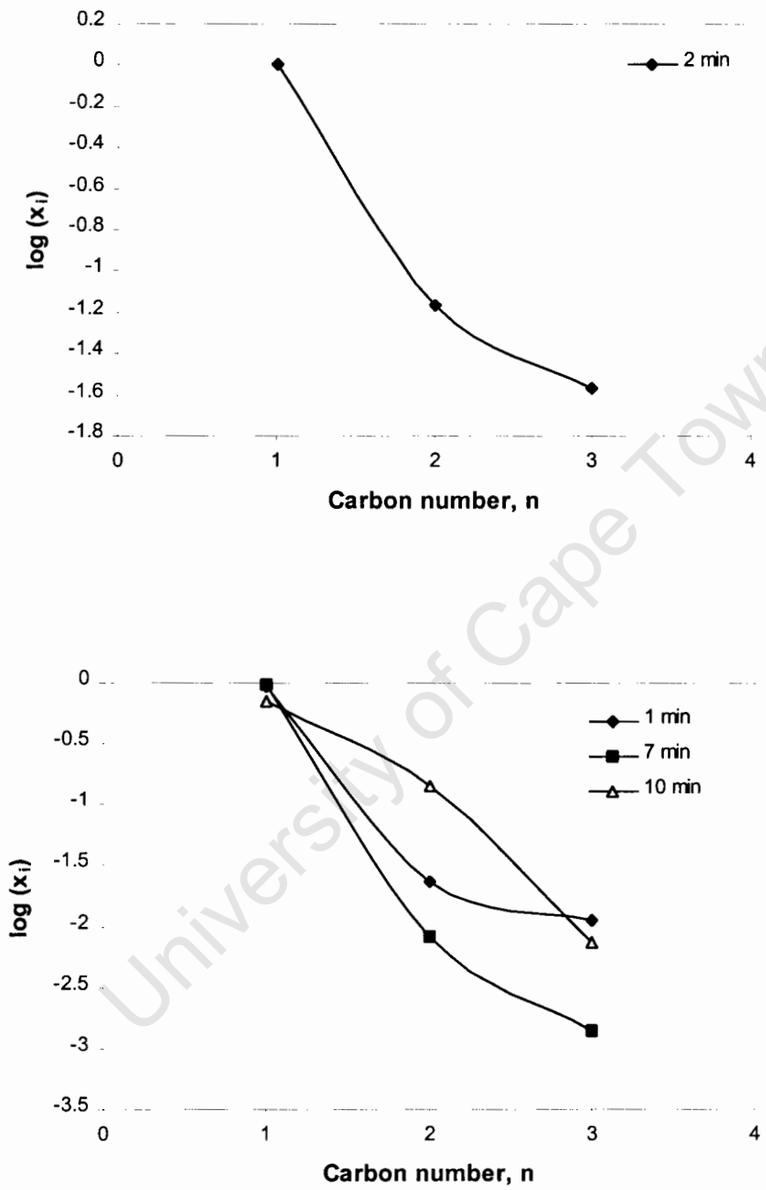

Figure 3.13: ASF distribution of FTS using $Os_3(CO)_{12}/SiO_2$ at 170 and 220 °C.

The ASF plots obtained at 170 and 220 °C in Figure 3.13 are quite similar and they follow the general trend, which has been observed in other syntheses. In the study by Claeys et al. carried out with the analogous $Ru_3(CO)_{12}/SiO_2$, similar results were obtained. The calculated chain growth probabilities for the $Os_3(CO)_{12}/SiO_2$ complex after 2 min TOS at 170 °C was found to be 0.17 and at 220 °C to be 0.11, 0.038 and 0.10. These values are very low, as expected, at both temperatures when compared to those for the standard Os/SiO_2 catalyst.

Figure 3.14 is a representation of two gas chromatograms obtained after 2 min and 1 min TOS at 170 and 220 °C, respectively. Visibility of C_2-and C_3-hydrocarbons in addition to methane is noticed.

(a)

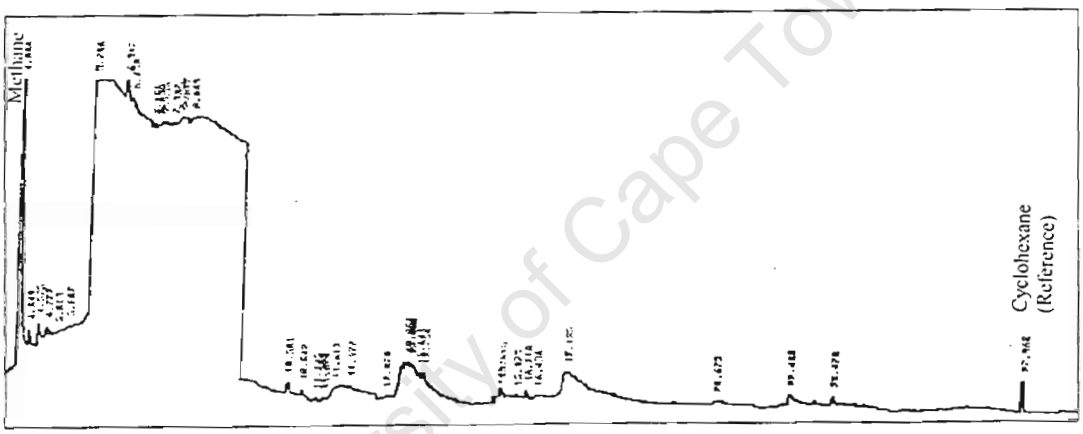

(b)

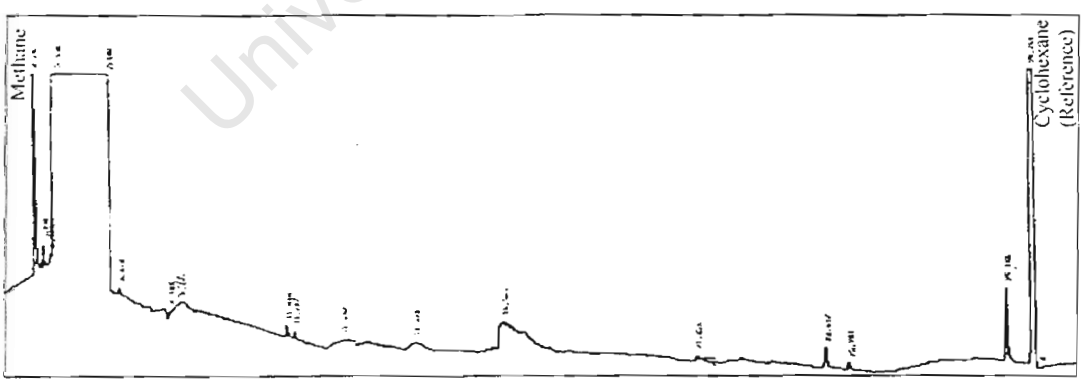

Figure 3.14: Comparison of gas chromatograms obtained using $Os_3(CO)_{12}/SiO_2$ at:(a) 170 °C and (b) 220 °C

The chain growth probabilities for the osmium (Table 3.1 and 3.2) and ruthenium (Table 3.3) complexes are summarised below, respectively. Generally, the chain growth probability decreases with increasing temperature and these values support this statement. Judging from these results, it is clear that all the catalysts obey the Anderson-Schulz-Flory distribution, since the α values are all between 0 and 1 ($0 \leq \alpha \leq 1$).

Table 3.1: α values at different reaction times for the CO hydrogenation with osmium compounds at 170 °C.

Complex	α_1	α_2	α_3
Standard Os/SiO_2	0.62	0.43	0.23
$[CpOs(CO)_2]_2/SiO_2$	0.12	0.056	0.39
$Os_3(CO)_{12}/SiO_2$	0.17	-	-

Table 3.2: α values for the CO hydrogenation with osmium compounds at 220 °C.

Complex	α_1	α_2	α_3
Standard Os/SiO_2	0.59	0.40	0.21
$[CpOs(CO)_2]_2/SiO_2$	0.083	0.075	0.083
$Os_3(CO)_{12}/SiO_2$	0.11	0.038	0.10

Table 3.3: α values for the CO hydrogenation with ruthenium compounds at 170 °C.

Complex	α_1	α_2	α_3
Standard Ru/SiO_2	0.68	0.42	0.56
$[CpRu(CO)_2]_2/SiO_2$	0.16	0.19	0.15
$Ru_3(CO)_{12}/SiO_2$ [54]	0.13	0.13	0.13

The α values obtained for the osmium complexes are less in comparison with those obtained for the ruthenium complexes.

3.4.5 Olefin to paraffin ratios of the C_2- and C_3- fraction

Table 3.4 shows the olefin : paraffin ratios for the C_2- and C_3- fractions at 170 °C. Clearly, for the standard Os/SiO_2 the C_2 fraction is higher than the C_3 fraction, a similar trend observed with the standard Ru/SiO_2. It is interesting to note also that these ratios obtained with osmium are significantly lower than the ones obtained with ruthenium. Based on these results, it is clear that ruthenium is more selective than osmium.

Table 3.4 Olefin : paraffin ratios for the osmium complexes at 170 °C.

Complex	C_2-fraction	C_3-fraction
Standard Os/SiO_2	0.53	0.88
$[CpOs(CO)_2]_2/SiO_2$	2.11	1.80
$Os_3(CO)_{12}/SiO_2$	1.54	1.31

3.5 Conclusions

It can be concluded from this above study that osmium is indeed active in Fischer-Tropsch synthesis but to a lesser extent than ruthenium. In terms of selectivity, ruthenium is more FT selective to long chain hydrocarbons than osmium. The osmium complexes seem to be more stable than the ruthenium complexes even at temperatures higher than 170 °C.

In both syntheses, it is believed that the carbonyl groups from the complexes serve as an alternative source for carbon whereas in the case of the base catalysts, the carbon monoxide from the feed is the only source of carbon since these do not have any CO groups.

At this point, it is not yet clear whether the ruthenium and osmium complexes did serve as catalysts. However, in particular $[Ru_2(CO)_2(\mu\text{-}CO)(\mu\text{-}CHMe)(\eta^5\text{-}C_5H_5)_2]/SiO_2$ showed promising results, as even after 1 hour steady product formation could be detected.

CHAPTER 4
EXPERIMENTAL

4.1 General

Reagents

Triruthenium dodecacarbonyl was purchased from Strem Chemicals. Butyllithium, $[(C_6H_5)_3C][PF_6]$, $NaBH_4$, triethyl amine and $HBF_4{\cdot}OEt_2$ were obtained from Sigma Aldrich. $Si[(CH_2)_3Si(CH_3)_2CH_2Cl]_4$ and $Si[(CH_2)_3Si(CH_3)_2CH_2Cl]_4$ [50] were prepared by literature methods. $RuCl_3.2H_2O$ was purchased from Sigma Aldrich. $(NH_4)_2OsCl_6$ and $Os_3(CO)_{12}$ were prepared by Prof. J. R. Moss. Alumina (Merck, 90, active, neutral) was deactivated prior to use. SiO_2 (Davisil^{TM}, grade 646, dp = 200-250 μm, dpore = 150 Å) was obtained from Merck.

Tetrahydrofuran (THF) and heptane were distilled from sodium. Acetone and dichloromethane were distilled from anhydrous $CaCl_2$.

Instruments

All reactions were carried out under nitrogen using standard Schlenk techniques. Melting points were recorded on a Kofler hot-stage microscope (Reicher Thermovar). Infrared spectra were recorded on a Perkin-Elmer Paragon 1000 FT-IR spectrometer in solution cells with NaCl plates in CH_2Cl_2 or hexane. The ^1H NMR spectra were recorded on either a Varian Mercury 300 MHz spectrometer or a Varian Unity 400 MHz spectrometer at room temperature and the chemical shifts were referenced internally using the residual proton impurities in the solvent ($CDCl_3$: δ = 7.27 ppm) and are reported relative to TMS (δ = 0.00 ppm). ^{13}C NMR spectra were recorded using the same instruments operating at 75 and 100 MHz, respectively and were referenced internally to the solvent resonance ($CDCl_3$: δ = 77.0 ppm) and are reported relative to TMS (δ = 0.00 ppm). The microanalytical laboratory at the University of Cape Town carried out the elemental analyses using the Fisons EA 1108 elemental analyser.

4.2 Experimental details

Synthesis of $[CpRu(CO)_2]_2$ [42]

Triruthenium dodecacarbonyl (1.00 g, 2.3 mmol) and freshly distilled cyclopentadiene (2.20 g, 17 mmol) in dry deoxygenated heptane (44 ml) were heated under reflux for 2h. After addition of heptane (38 ml), the mixture was heated under reflux for a further 2 h. The mixture was allowed to cool at room temperature and was then left for 2 days at 0 °C to allow crystallization. The brown product (0.402 g) was filtered. The solvent was then removed from the filtrate *in vacuo* followed by chromatography on an alumina (Brockman grade 2) column. Elution of the yellow band with ethylacetate-hexane (1:3) afforded a brown solid (0.207 g, 30 %), m.p. 185-188 °C. Found: C, 37.57; H, 2.15 %. $C_{14}H_{10}O_4Ru_2$ requires C, 37.8; H, 2.1. ν_{max}/cm^{-1} (CO) 2023s, 2004w, 1959s, 1938 (sh) and 1770m (CH_2Cl_2) (lit. 2003s, 1966s, 1934m and 1771s); δ_H ($CDCl_3$, 200MHz) 5.278 (10 H, s, C_5H_5); δ_C ($CDCl_3$, 100 MHz) 216.5 (CO), 89.00 ($\underline{C}_5H_5$).

Synthesis of $[Cp^*Ru(CO)_2]_2$ [43]

A mixture of $Ru_3(CO)_{12}$ (0.517 g, 0.81 mmol) and C_5Me_5 (0.350 g, 2.70 mmol) in n-decane (20 ml) was heated under reflux for 4 h. The temperature was allowed to reach room temperature during 12 h and the clear red solution gave orange-red crystals (0.402 g), which were then filtered. Recrystallization from a mixture of dichloromethane and hexane gave (0.315 g, 67 %) m.p. 280 °C (dec.) (lit. 297 °C (dec)). Found: C, 48.72; H, 5. 26 %. $C_{24}H_{30}O_4Ru_2$ requires C, 49.3; H, 5.1 %. ν_{max}/cm^{-1} (CO) 1925s and 1744s (CH_2Cl_2) (lit. 1925s and1744s); δ_H ($CDCl_3$, 200MHz) 1.837 (15 H, s, C_5Me_5); δ_C ($CDCl_3$, 100 MHz) 202.6 (CO), 101.2 ($\underline{C}_5(CH_3)_5$), 9.2 ($C_5(\underline{C}H_3)_5$).

Synthesis of $[Ru_2(CO)_2(\mu\text{-}CO)(\mu\text{-}CHMe)(\eta^5\text{-}C_5H_5)_2]$ [42]

BuLi (1.2 ml of 1.6 M solution) was added by syringe to a solution of tetracarbonylbis(η^5-cyclopentadienyl)diruthenium (0.500 g, 1.13 mmol) in THF (20 ml). The mixture was stirred for 1 h and then cooled to –78 °C. An excess of $HBF_4{\cdot}OEt_2$ (1 ml) was added and the mixture was stirred for 30 min at this temperature. To the mixture, an excess of $NaBH_4$ (0.25 g, 6.58 mmol) was added and

the temperature was allowed to reach room temperature during 30 min. The solution was then concentrated under reduced pressure and the product was extracted with dichloromethane. The extracts were filtered through a short alumina column followed by chromatography on another alumina (Brockman grade 2) column. Elution with dichloromethane-hexane (1:1) gave a yellow solid (0.14 g, 32 %) m.p. 228-230 °C. Found: C, 40.29; H, 3.20 %. $C_{15}H_{14}O_3Ru_2$ requires C, 40.5; H, 40.5 %. ν_{max}/cm^{-1} (CO) 1974s, 1933m and 1776m (CH_2Cl_2) (lit. 1974s, 1933m and 1776m); δ_H ($CDCl_3$, 200MHz) trans isomer 3.03 (3H, d, *J*(CH) 7Hz, μ-CH**Me**), 5.18 (5H, s, C_5H_5), 5.29 (5H, s, C_5H_5) and 10.97 (1H, q, *J*(CH) 7 Hz, μ-C**H**Me); cis isomer 3.02 (3H, d, *J*(CH) 7Hz, μ-CH**Me**), 5.18 (10H, s, $2C_5H_5$) and 10.97 (1H, q, *J*(CH) 7 Hz, μ-C**H**Me); δ_C ($CDCl_3$, 100 MHz) 203.5 (CO), 89.5 ($\underline{C}_5H_5$), 49.8 ($\underline{C}HCH_3$), 30.2 ($CH\underline{C}H_3$).

Attempted synthesis of $Si[(CH_2)_3Si(CH_3)_2CH_2I]_4$

A mixture of $Si[(CH_2)_3Si(CH_3)_2CH_2Cl]_4$ (0.500 g, 8.01 mmol), potassium iodide (1.00 g, 6.03 mmol) and acetone (20 ml) was heated under reflux for 24 h. A white solid precipitate was observed and the volatiles were removed *in vacuo*. The remaining solids were partitioned between hexane (25 ml) and water (25 ml). The aqueous layer was extracted with hexane (3 x 25 ml). The combined organic layers were washed with water (3 x 25 ml) and brine (3 x 25 ml), dried over $MgSO_4$ and then filtered. After removal of volatiles *in vacuo* the remaining solid was identified as unreacted starting material by ^1H NMR spectroscopy.

Attempted synthesis of 2Ru-Rp3G1C

A mixture of $Si[(CH_2)_3Si(CH_3)_2CH_2Br]_4$ (0.500 g, 6.22mmol), tetracarbonylbis(η^5-cyclopentadienyl)diruthenium (1.00 g, 2.25 mmol), dry deoxygenated THF (40 ml) and MeLi in diethylether (2.3 ml of 1 M solution) was stirred for 1h and then cooled to –78 °C. An excess of $HBF_4 \cdot OEt_2$ (2 ml) was added and the mixture was stirred at this temperature for 30 min followed by the addition of an excess of $NaBH_4$ (0.5 g, 13.3 mmol). The mixture was then allowed to warm to room temperature over 30 min, followed by evaporation of the solvent at reduced pressure. The residue was extracted with dichloromethane (100 ml) and the extracts were filtered. Analysis by ^1H NMR showed no formation of the desired product.

Synthesis of $[Os(CO)_3Cl_2]_2$

$(NH_4)_2OsCl_6$ (2.00 g, 4.59 mmol) and ethanol (60 ml) were placed in a stainless steel autoclave. After it was sealed, the autoclave was purged twice with CO (36 bar) and was then pressurised with CO (70 bar) while stirring continuously. After 5 min the pressure was checked to see if it holds up and the autoclave was heated to 175 °C. The pressure was recorded hourly and the reaction was carried out for 21 h. Following cooling and depressurisation, the contents of the autoclave were removed. Removal of the solvent *in vacou* afforded a yellow oil (1.87 g, 59 %). ν_{max}/cm^{-1} (CO) 2028s and 2119s (CH_2Cl_2).

Synthesis of $[CpOs(CO)_2H]$ [48]

To a solution of NaC_5H_5 (2.50 g, 28 mmol) in THF (50 ml), a solution of $[Os(CO)_3Cl_2]_2$ (1.20 g, 1.74 mmol) in 50 ml of the same solvent was added dropwise over 15 min. The mixture was then stirred for 16 h at room temperature. After removal of the solvent *in vacuo* the remaining solid was extracted with dichloromethane and then filtered in a fluted filter paper. The solvent was removed from the filtrate, resulting in a brown oil (0.48g, 88 %). ν_{max}/cm^{-1} (CO) 2020s, 1959s and 2087wbr (hexane) (lit. 2020s, 1960s and 2089wbr) [51]; δ_H ($CDCl_3$, 400MHz) 5.39 (5H, s, C_5H_5), -14,50 (1H, s, OsH).

Synthesis of $[CpOs(CO)_2]_2$ [48]

A solution of $[(C_6H_5)_3C][PF_6]$ (181 mg, 0.65 mmol) in CH_2Cl_2 (2 ml) was added to a solution of $[CpOs(CO)_2H]$ (291 mg, 0.93 mmol) in 25 ml of the same solvent. The mixture was stirred for 2h at room temperature. Triethyl amine (2 ml) was then added to the brown mixture and after drawing off the solvent under vacuum the resulting residue was chromatographed on silica. The impurities were eluted with hexane and the brown product was obtained by eluting the yellow band with dichloromethane (262 mg, 45 %). Found: C, 27.00; H, 1.54 %. $C_{14}H_{10}O_4Os_2$ requires C, 26.89; H, 1.57 %. ν_{max}/cm^{-1} (CO) 2020vs, 1961vs, 2041s and 1988s (hexane) (lit. 1915vs and 1960vs (KBr)); δ_H ($CDCl_3$, 400MHz) 4.86 (5H, s, C_5H_5); δ_C ($CDCl_3$, 100 MHz) 218.3 (CO), 90.2 ($\underline{C}_5H_5$).

4.3 Catalytic CO hydrogenation experiments

4.3.1 Preparation of catalysts

Preparation of the standard Ru/SiO_2

$RuCl_3.2H_2O$ (0.03 g) was dissolved in water (5 ml) in a small beaker and stirred. The solution was then contacted with SiO_2 (1.00 g). The impregnated sample was dried at room temperature in air for 2 h and was further dried at 110 °C for 4 h to give a black solid.

Preparation of $[CpRu(CO)_2]_2/SiO_2$

To a solution of $[CpRu(CO)_2]_2$ (0.067 g) in acetone (5 ml), SiO_2 (1.00 g) was added. The solvent was removed by gently blowing N_2 over the mixture at room temperature and was left to dry in air. A brown solid was obtained.

Preparation of $[Cp^*Ru(CO)_2]_2/SiO_2$

$[C_5Me_5Ru(CO)_2]_2$ (0.1127 g) was dissolved in acetone (5 ml) and to the solution SiO_2 (1.00 g) was added. The mixture was then dried completely and an orange solid was obtained.

Preparation of $[Ru_2(CO)_2(\mu\text{-}CO)(\mu\text{-}CHMe)(\eta^5\text{-}C_5H_5)_2]/SiO_2$

SiO_2 (1.00 g) was added to a solution of $[Ru_2(CO)_2(\mu\text{-}CO)(\mu\text{-}CHMe)(\eta^5\text{-}C_5H_5)_2]$ (0.067 g) in acetone (5 ml) and the mixture was dried in air at room temperature and it afforded a yellow solid.

Preparation of the standard Os/SiO_2

$(NH_4)_2OsCl_6$ (0.0693 g) was dissolved in water (5 ml) in a small beaker and stirred. The solution was then contacted with SiO_2 (1.00 g) and the impregnated sample was dried at room temperature in air for 2 h and was further dried at 110 °C for 4 h. A brick-red solid was obtained.

Preparation of $[CpOs(CO)_2]_2/SiO_2$

To a solution of $[CpOs(CO)_2]_2$ (0.0491 g) in acetone (5 ml), SiO_2 (1.00 g) was added. The solvent was removed by gently blowing N_2 over the mixture at room temperature and was left to dry in air, affording a brown solid.

Preparation of $Os_3(CO)_{12}/SiO_2$

SiO_2 (1.00 g) was added to a solution of $Os_3(CO)_{12}$ (0.0477 g) in acetone (5 ml) and the mixture was dried in air at room temperature. A yellow solid was obtained.

4.3.2 Experimental apparatus

The experimental set-up used for the CO hydrogenation experiments is shown in Figure 4.1. The apparatus was designed to detect the initial behaviour of each catalyst used and to separate FT activity from disintegration of the Ru or Os complexes.

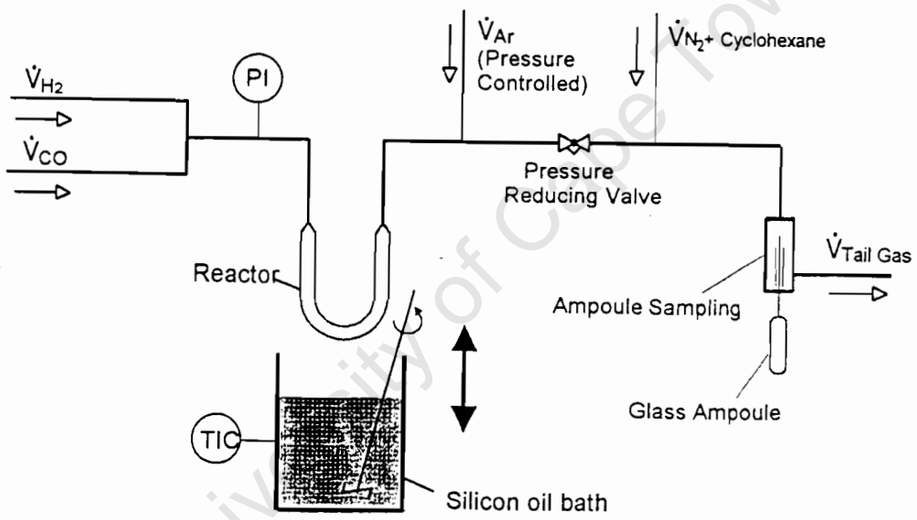

Figure 4.1: Schematic of the experimental set-up used for CO hydrogenation.

A small stainless steel U-tube flow reactor (internal volume = 1.5 ml) was used to carry out the catalytic experiments. Syngas ($CO + H_2$) is passed through the reactor at stoichiometric ratio (2 H_2 : 1 CO). A reference gas stream (N_2 and cyclohexane) is

mixed with the product stream and it serves as an internal standard. The volumetric flow rates of the gases were controlled using mass flow controllers. The total temperature and pressure of the system are kept constant at 170 °C and 2 bar, respectively. Gas samples are taken using the rapid ampoule sampling technique, which allows a high number of samples to be taken in a short space of time. Analysis of the samples was done using a gas chromatograph.

Catalyst packing

The right leg of the reactor was filled with 0.4 g of the catalyst and SiC was loaded (~1 g) into the left leg (see Figure 4.1). These two were separated from each other by a glasswool. The main purpose of loading SiC is to preheat the syngas before it reaches the catalyst bed. The remaining space in both legs was filled with glass wool to ensure that the bed is fixed.

Reaction start-up

The reactor was inserted into the rig and pressure testing was done to check if there were any leaks in the system.

Prior to the synthesis, the standard catalysts were reduced in H_2 (30 ml (NTP)/min and the temperature was set at 300 °C. The reduction (heating rate 4°C/min) was carried out for 5 h. The reactor was placed in a metal casing and a thermocouple was inserted to monitor the temperature. Glass wool was used to cover the casing to prevent loss of heat. The complexes were not pretreated.

The silicon oil bath was heated to reaction temperature. Flow rates were set using mass flow controllers. H_2 was set at 6 ml/min, CO at 3 ml/min and the reference gas (a mixture of CH_x and nitrogen) at 3 ml/min. The ratio of H_2:CO was kept at 2:1 and this was checked using GC (TCD).

After reduction of the catalyst the reactor was cooled. FT-synthesis was started by dipping the reactor into the silicon oil bath and the samples were taken using ampoules, initially at 20s intervals and then later hourly over the 24 h period.

Ampoule Sampling Technique

The evacuated glass ampoules were prepared by sealing off the capillary end of the pasteur pipette with a flame, filling the other end with vacuum and then sealing it off. Gas samples were taken by inserting the capillary end through a rubber septum and then pushed gently right through to the end of the tube (Figure 4.2). When the end point had been reached the tip of capillary was broken and the gas was allowed to rush in. The ampoule was then pulled slightly and sealed with a flame. The sample was then later analysed with GC (FID).

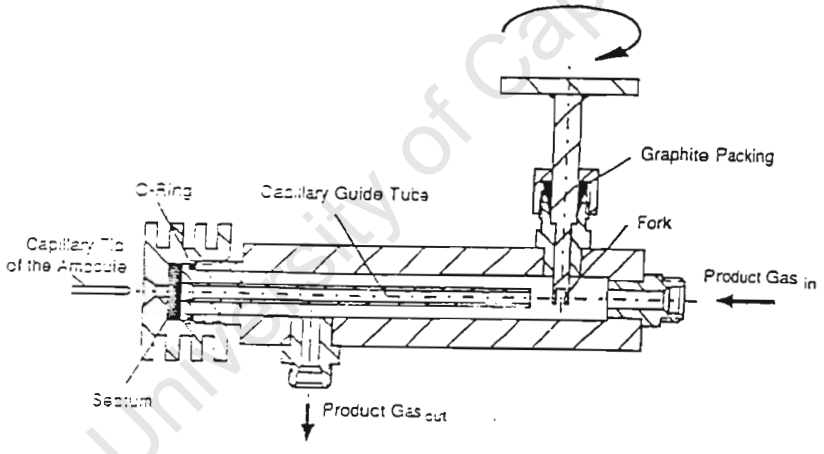

Figure 4.2: Ampoule sampler

Gas Chromatograph Analysis

Inorganic gases (H_2, CO, CO_2, N_2) and methane were analysed using a gas chromatograph (Varian 3700) with a packed column (3m x $1/8^n$, Carbosieve II) and a thermal conductivity detector (TCD). For the analysis of the organic products,

Varian 3400 gas chromatograph with a flame ionisation detector (FID), and a 50m x 0.25 mm x 0.5 μm fused silica capillary column (Chrompak CP-Sil 5 CB) at temperature program: -68 to 280 ºC was used.

REFERENCES

1. F. Fischer and H. Tropsch, *Brennst. Chem.*, **1926**, 7, 97.
2. M. E. Dry, *Appl. Catal. A: Gen.*, **1996**, 138, 319.
3. P. M. Maitlis, Q. Ruhksana, H. C. Long and M. L. Turner, *Appl. Catal. A: Gen.*, **1999**, 186, 363.
4. M. E. Dry, *Catal. Today*, **2002**, 71, 227.
5. M. J. Overett, R. O. Hill and J. R. Moss, *Coord. Chem. Rev.*, **2000**, 206, 581.
6. M. L. Turner, N. Marsih, B. E. Mann, R. Quyoum, H. C. Long and P. M. Maitlis, *J. Am. Chem. Soc.*, **2002**, 35, 10456.
7. J. H. Lunsford, *Catal. Today*, **2000**, 63, 165.
8. M. A. Vannice, *J. Catal.*, **1977**, 50, 228.
9. M. Claeys and E. van Steen, *Catal. Today*, **2002**, 71, 419.
10. W. A. Herrmann and B. Cornils, *Angew. Chem., Int. Ed.*, **1997**, 36, 1048.
11. G. W. Parshall and R. E. Putscher, *J. Chem. Educ.*, **1986**, 63, 189.
12. M. A. Hearshaw, PhD Thesis, University of Cape Town, **1999**.
13. M. Reinikainen, M. K. Niemela, N. Kakuta and S. Suhonen, *Appl. Catal. A: Gen.*, **1998**, 174, 61.
14. R. C. Reuel and C. H. Bartholomew, *J. Catal.*, **1984**, 85, 63.
15. P. Johnston, G. J. Hutchings, N. J. Coville, K. P. Finch and J. R. Moss, *Appl. Catal. A: Gen.*, **1999**, 186, 245.
16. G. C. Bond, *A. Chem. Res.*, **1993**, 26, 490.
17. R. A. Sanchez-Delgado, J. S. Bradley and G. Wilkinson, *J. Chem. Soc., Dalton Trans.*, **1976**, 399.
18. B. R. James and L. D. Markham, *J. Catal.*, **1972**, 27, 442.
19. G. Strathdee and R. M. Given, *Can. J. Chem.*, **1975**, 53, 106.
20. P. G. Jessop, T. Ikariya and R. Noyori, *Nat. (Lond.)*, **1994**, 368, 231.
21. J. H. Köhler and H. L. Krauss, *J. Mol. Catal. A: Chem.*, **1997**, 123, 49.
22. P. Psaro and S. Recchia, *Catal. Today*, **1998**, 41, 139.
23. J. Robertson and G. Webb, *Proc. R. Soc. Lond. A*, **1974**, 341, 383.
24. M. Vinigera, R. Gomez and R.D. Gonzalez, *J. Catal.*, **1988**, 111, 429.
25. S. I. Niva, F. Mizukami, M. Kuno, T. Takeshita, H. Nakamura, T. Tsuchiya, K. Shimizu and J. Imamura, *J. Mol. Catal.*, **1986**, 34, 247.

26. M. A. Vannice, *J. Catal.*, **1975**, 37, 449.
27. R. C. Brady III, R. J. Pettit, *J. Am. Chem. Soc.*, **1980**, 102, 6181.
28. P. Biloen, *J. Neth. Chem. Soc.*, **1980**, 99, 33.
29. H. Schulz, *Appl. Catal. A: Gen.*, **1999**, 186, 3.
30. P. M. Maitlis, H. C. Long, R. Quyoum, M. L. Turner and Z. Q. Wang, *J. Chem. Soc., Chem. Commun.*, **1996**, 1.
31. S. B. Ndlovu, N. S. Phala, M. Hearshaw-Timme, P. Beagley, J. R Moss, M. Claeys and E. van Steen, *Catal. Today*, **2002**, 71, 343.
32. H. Pichler, H. Schulz, *Chem. –Ing. –Techn.*, **1970**, 42, 1162.
33. B. H. Davis, *Fuel Proc. Techn.*, **2001**, 71, 157.
34. L. Nowicki, S. Ledakowicz and D. B. Bukur, *Chem. Eng. Sci.*, **2001**, 56, 1175.
35. H. Pichler, H. Schulz and M. Elstner, *Brennst. Chem.*, **1967**, 48, 78.
36. R. J. Madon and W. F. Taylor, *J. Catal.*, **1981**, 69, 32.
37. G. A. Huff and C. N. Satterfield, *J. Catal.*, **1984**, 85, 370.
38. L. Kőnig and J. Gaube, *Chem. Ing. Technol.*, **1983**, 55, 14.
39. E. Iglesia, S. C. Reyes and R. J. Madon, *J. Catal.*, **1991**, 129, 238.
40. J. Patzlaff, Y. Liu, C, Graffmann and J. Gaube, *Catal. Today*, **2002**, 71, 381.
41. R. Gómez-Garcia and P. Royo, *J. Organomet. Chem.*, **1999**, 583, 86.
42. N. M. Doherty and S. A. R. Knox, *Inorg. Synth.*, **1989**, 25, 179.
43. R. B. King, M. Z. Iqbal and A. D. King Jr., *J. Organomet. Chem.*, **1979**, 171, 53.
44. M. Claeys, M. Timme, M. Overett, J. R. Moss and E. van Steen, *Stud. Surf. Sci. Catal.*, **2000**, 130, 1157.
45. R. B. Anderson, *The Fischer-Tropsch Synthesis*, Academic Press, New York, **1984**, pp. 174-225.
46. W. P. Griffith, *The Chemistry of the Rarer Platinum Metals (Os, Ru, Ir and Rh)*, Interscience, London, **1967**, pp.3-9; F. A. Cotton, G. Wilkinson, C. A Murillo and M. Bochmann, *Advanced Inorganic Chemistry*, Wiley, New York, **1999**.
47. W. A. Herrmann, E, Herdtweck and A. Schafer, *Chem. Ber.*, **1988**, 121, 1907.
48. W. Beck and K. Z. Schloter, *Naturforsch., B: Anorg. Chem., Org. Chem.*, **1978**, 33B, 1214.
49. A. Choplin, M. Leconte and J. M Basset, *J. Mol. Catal.*, **1983**, 21, 389.

50. D. De Groot, J. N. H. Reek, P. C. J. Kamer and P. W. N. M. van Leeuwen, *Eur. J. Org. Chem.*, **2002**, 6, 1085.
51. J. K. Hoyano, C. J. May and W. A. G. Graham, *Inorg. Chem.*, **1982**, 21, 3095.
52. R. H. Grubbs and S. Chang, *Tet. Lett.*, **1998**, 54, 4413.
53. R. Baum, *C & EN*, **2003**, 81, (36), 112.
54. M. Claeys, M. Hearshaw-Timme, J. R. Moss and E. van Steen, *DGMK-Conference, Dresden, Germany,* **2000**, 10505, 95.
55. H. H. Storch, N. Golumbic and R. B. Anderson, *The Fischer Tropsch and Related Synthesis*, Wiley, New York, **1951**, 222.
56. R. B. Anderson, R. A Friedel and H. H. Storch, *J. Chem. Phys.*, **1951**, 19, 313.